

Study of Z production in PbPb and pp collisions at $\sqrt{s_{NN}} = 2.76$ TeV in the dimuon and dielectron decay channels

Journal Article

Author(s):

CMS Collaboration; Chatrchyan, Serguei; Bachmair, Felix; Bäni, Lukas; Bianchini, Lorenzo; Bortignon, Pierluigi; Buchmann, Marco A.; Casal, Bruno; Chanon, Nicolas; Deisher, Amanda; Dissertori, Günther; Dittmar, Michael; Donegà, Mauro; Dünser, Marc; Eller, Philipp; Grab, Christoph; Hits, Dmitry; Luster mann, Werner; Mangano, Boris; Marini, Andrea C.; Martinez Ruiz del Arbol, Pablo; Meister, Daniel; Mohr, Niklas; Nägeli, Christoph; Nessi-Tedaldi, Francesca; Pandolfi, Francesco; Pauss, Felicitas; Peruzzi, Marco; Quittnat, Milena; Rebane, Liis; Rossini, Marco; Starodumov, Andrey; Takahashi, Maiko; Theofilatos, Konstantinos; Wallny, Rainer; Weber, H.A.; et al.

Publication date:

2015-03

Permanent link:

<https://doi.org/10.3929/ethz-b-000099663>

Rights / license:

[Creative Commons Attribution 4.0 International](#)

Originally published in:

Journal of High Energy Physics 2015(3), [https://doi.org/10.1007/JHEP03\(2015\)022](https://doi.org/10.1007/JHEP03(2015)022)

Study of Z production in PbPb and pp collisions at $\sqrt{s_{NN}} = 2.76$ TeV in the dimuon and dielectron decay channels



The CMS collaboration

E-mail: cms-publication-committee-chair@cern.ch

ABSTRACT: The production of Z bosons is studied in the dimuon and dielectron decay channels in PbPb and pp collisions at $\sqrt{s_{NN}} = 2.76$ TeV, using data collected by the CMS experiment at the LHC. The PbPb data sample corresponds to an integrated luminosity of about $166 \mu\text{b}^{-1}$, while the pp data sample collected in 2013 at the same nucleon-nucleon centre-of-mass energy has an integrated luminosity of 5.4pb^{-1} . The Z boson yield is measured as a function of rapidity, transverse momentum, and collision centrality. The ratio of PbPb to pp yields, scaled by the number of inelastic nucleon-nucleon collisions, is found to be 1.06 ± 0.05 (stat) ± 0.08 (syst) in the dimuon channel and 1.02 ± 0.08 (stat) ± 0.15 (syst) in the dielectron channel, for centrality-integrated Z boson production. This binary collision scaling is seen to hold in the entire kinematic region studied, as expected for a colourless probe that is unaffected by the hot and dense QCD medium produced in heavy ion collisions.

KEYWORDS: Particle and resonance production, Heavy Ions, Heavy-ion collision, proton-proton scattering

ARXIV EPRINT: [1410.4825](https://arxiv.org/abs/1410.4825)

Contents

1	Introduction	1
2	The CMS detector	2
3	Event selection and centrality determination	3
4	Lepton reconstruction	4
5	Signal extraction, corrections, and systematic uncertainties	5
5.1	Signal extraction	5
5.2	Acceptance and efficiency	6
5.3	Systematic uncertainties	8
6	Results	10
6.1	Z boson production cross section in pp collisions	10
6.2	Z boson yields in PbPb collisions vs. p_T , y , and centrality	10
6.3	Nuclear modification factor	12
6.4	Combined results for the two decay channels	14
7	Summary	16
	The CMS collaboration	23

1 Introduction

The Z boson was first observed by the UA1 and UA2 experiments at CERN in proton-antiproton collisions at a centre-of-mass energy of 540 GeV [1, 2]. Since then, its properties have been characterized in detail by a succession of collider experiments [3–10]. These properties, including mass and decay widths, as well as inclusive and differential cross sections, have been measured at different centre-of-mass energies in electron-positron, proton-proton, and proton-antiproton collisions. The large centre-of-mass energy and substantial integrated luminosities delivered by the CERN LHC for Pb beams provide new opportunities to study Z boson production in nucleus-nucleus collisions.

The Z bosons decay with a typical lifetime of 0.1 fm/c and their leptonic decays are of particular interest since leptons pass through the medium being probed without interacting strongly. Dileptons from Z boson decays can thus serve as a control for the processes expected to be heavily modified in the hot and dense medium, such as quarkonium or Z+jet production [11]. However, in heavy ion collisions, Z boson production can be affected by initial-state effects. The modification of the yield in heavy ion collisions is expected to be about 3% from isospin effects, the result of the proton-neutron (or u-d quark) ratio being different in protons and Pb nuclei [12], and from multiple scattering and energy loss of the

initial partons [13]. In addition, the nuclear modification of parton distribution functions (PDF) can lead to rapidity-dependent changes on the order of up to 5% in the observed Z boson yield in PbPb collisions [12].

Based on the first PbPb collisions at the LHC, with an integrated luminosity of about $7 \mu\text{b}^{-1}$, the CMS collaboration reported results on the $Z \rightarrow \mu^+\mu^-$ [14], $W^\pm \rightarrow \mu^\pm\nu$ [15] and isolated photon [16] production. These measurements show that electroweak bosons are essentially unmodified by the hot and dense medium. In this paper, Z boson production at $\sqrt{s_{\text{NN}}} = 2.76 \text{ TeV}$ is studied using PbPb collision data collected in 2011, which corresponds to an integrated luminosity of about $166 \mu\text{b}^{-1}$. From this PbPb data-taking period, the ATLAS collaboration published Z boson yields showing no deviation with respect to theoretical predictions [17]. The set of pp data at the same centre-of-mass energy recorded in 2013 by CMS, with a total integrated luminosity of 5.4 pb^{-1} , is used to measure pp yields. The nuclear modification factor (R_{AA}), the ratio of PbPb and pp yields scaled by the number of inelastic nucleon-nucleon binary collisions, is then calculated. These larger PbPb and pp data samples allow a more precise measurement of the Z boson yield dependence on transverse momentum (p_{T}), rapidity (y), and collision centrality. The dimuon channel is analyzed with an improved reconstruction algorithm (described in section 4) compared to ref. [14], and the electron channel is used for the first time in CMS to measure Z boson production in heavy ion collisions.

2 The CMS detector

The central feature of the CMS apparatus is a superconducting solenoid of 6 m internal diameter, providing a magnetic field of 3.8 T. Within the superconducting solenoid volume are a silicon pixel and strip tracker, a lead tungstate crystal electromagnetic calorimeter (ECAL), and a brass/scintillator hadron calorimeter (HCAL), each composed of a barrel and two endcap sections. Muons are measured in gas-ionization detectors embedded in the steel flux-return yoke outside the solenoid. Extensive forward calorimetry complements the coverage provided by the barrel and endcap detectors. A more detailed description of the CMS detector, together with a definition of the coordinate system used and the relevant kinematic variables, can be found in ref. [18].

Muons are measured in the pseudorapidity range $|\eta| < 2.4$ using three technologies: drift tubes, cathode strip chambers, and resistive-plate chambers. Matching muons to tracks measured in the silicon tracker results in a relative transverse momentum resolution for muons with $20 < p_{\text{T}} < 100 \text{ GeV}$ of 1.3–2.0% in the barrel and better than 6% in the endcaps. The p_{T} resolution in the barrel is better than 10% for muons with p_{T} up to 1 TeV [19]. Electrons are measured in the ECAL that consists of 75 848 lead tungstate crystals providing a pseudorapidity coverage in the barrel region (EB) of $|\eta| < 1.48$ and in the two endcap regions (EE) of $1.48 < |\eta| < 3.0$. The ECAL energy resolution for electrons with a transverse energy $E_{\text{T}} \approx 45 \text{ GeV}$, which is typical of $Z \rightarrow e^+e^-$ decays, is better than 2% in the central region of the ECAL barrel ($|\eta| < 0.8$), and is between 2% and 5% elsewhere. For low-bremsstrahlung electrons, where 94% or more of their energy is contained within a 3×3 array of crystals, the energy resolution improves to 1.5% for $|\eta| < 0.8$ [20]. Matching ECAL clusters to tracks measured in the silicon tracker is used

to differentiate electrons from photons. Two steel/quartz-fiber Cherenkov hadron forward calorimeters (HF) are used to estimate the centrality of the PbPb collisions. The HF detectors are located on each side of the interaction point, covering the pseudorapidity region $2.9 < |\eta| < 5.2$.

3 Event selection and centrality determination

In order to select a sample of purely inelastic hadronic PbPb collisions, the contamination from ultraperipheral collisions and non-collision beam background is removed, as described in ref. [21]. Events are preselected if they contain a reconstructed primary vertex containing at least two tracks and at least three HF towers on each side of the interaction point with an energy of at least 3 GeV deposited in each tower. To further suppress the beam-gas events, the distribution of hits in the pixel detector along the beam direction is required to be compatible with particles originating from the event vertex. These criteria select $(97 \pm 3)\%$ of hadronic PbPb collisions [21], corresponding to a number of efficiency-corrected minimum bias (MB) events $N_{\text{MB}} = (1.16 \pm 0.04) \times 10^9$ for the sample analyzed. The pp dataset corresponds to an integrated luminosity of 5.4 pb^{-1} known to an accuracy of 3.7% from the uncertainty in the calibration based on a van der Meer scan [22].

For the $Z \rightarrow \mu^+ \mu^-$ study in PbPb collisions, a trigger requiring a single muon with p_{T} greater than 15 GeV/c is used, while a double-muon trigger with no explicit p_{T} selection is used for the pp sample. The efficiency for triggering on the $Z \rightarrow \mu^+ \mu^-$ channel within the selection and the acceptance requirements of the analysis is approximately 99% and 98% in the case of PbPb and pp collisions, respectively. For the $Z \rightarrow e^+ e^-$ channel in both PbPb and pp collisions, a trigger requires two significant energy deposits in the ECAL, one with $E_{\text{T}} > 20 \text{ GeV}$ and another with $E_{\text{T}} > 15 \text{ GeV}$. The trigger efficiencies for the $Z \rightarrow e^+ e^-$ channel are approximately 96% and 99% for Z bosons produced in PbPb and pp collisions, respectively. The difference comes from the energy-clustering algorithms used at the trigger level in PbPb [23] and pp [24] collisions.

Centrality for PbPb collisions is defined by the geometrical overlap of the incoming nuclei, and allows for splitting up the PbPb data into centrality classes ranging from peripheral, where there is little overlap of the colliding nuclei, to central, where there is nearly complete overlap of the colliding nuclei. In CMS, the centrality of a PbPb collision is defined through bins that correspond to fractions of the total hadronic inelastic cross section as observed in the distribution of the sum of the transverse energy deposited in the HF calorimeters [21]. The centrality classes used in this analysis are 50–100% (most peripheral), 40–50%, 30–40%, 20–30%, 10–20%, and 0–10% (most central), ordered from the lowest to the highest HF energy deposit.

When measuring the nuclear modification factor, R_{AA} , as described in section 6.3, the corrected Z boson yields in PbPb collisions are compared to those in pp collisions, scaled by the nuclear overlap function, T_{AA} [25]. At a given centrality, T_{AA} can be interpreted as the NN-equivalent integrated luminosity per nucleus-nucleus (AA) collision, and T_{AA} -normalized Z boson yields can thus be directly compared with the Z boson production cross sections in pp collisions. In units of mb^{-1} , the average T_{AA} goes from 0.47 ± 0.07 to 23.2 ± 1.0 , from the peripheral 50–100% to the central 0–10% ranges. These numbers,

Centrality	$\langle N_{\text{part}} \rangle$	$\langle N_{\text{coll}} \rangle$	$\langle T_{\text{AA}} \rangle$ (mb $^{-1}$)
[50, 100]%	22 ± 2	30 ± 5	0.47 ± 0.07
[40, 50]%	86 ± 4	176 ± 21	2.75 ± 0.30
[30, 40]%	130 ± 5	326 ± 34	5.09 ± 0.43
[20, 30]%	187 ± 4	563 ± 53	8.80 ± 0.58
[10, 20]%	261 ± 4	927 ± 81	14.5 ± 0.80
[0, 10]%	355 ± 3	1484 ± 120	23.2 ± 1.00
[0, 100]%	113 ± 3	363 ± 32	5.67 ± 0.32

Table 1. The average numbers of participating nucleons (N_{part}), binary collisions (N_{coll}), and the nuclear overlap function (T_{AA}), corresponding to the centrality ranges used in this analysis.

as well as all centrality-related quantities summarized in table 1, are computed using the Glauber model [25, 26]. The same parameters are used as in ref. [21], namely standard parameters for the Woods-Saxon function that distributes the nucleons in the Pb nuclei, and a nucleon-nucleon inelastic cross section of $\sigma_{\text{NN}}^{\text{inel}} = 64 \pm 5$ mb, based on a fit to the existing data for total and elastic cross sections in proton-proton and proton-antiproton collisions [27]. It is to be noted that the PbPb hadronic cross section (7.65 ± 0.42 barns) computed with this Glauber Monte Carlo simulation results in an integrated luminosity of $152 \pm 9 \mu\text{b}^{-1}$ compatible within 1.2σ with the integrated luminosity based on the van der Meer scan which has been evaluated to be $166 \pm 8 \mu\text{b}^{-1}$. All the results presented in the paper have been obtained using the Glauber model and event counting that is equivalent to $152 \mu\text{b}^{-1}$ expressed in terms of luminosity.

4 Lepton reconstruction

Muons are reconstructed using a global fit to a track in the muon detectors matched to a track in the silicon tracker. The offline muon reconstruction algorithm used for the PbPb data has been significantly improved relative to that used for the previous measurement [14]. The efficiency has been increased by running multiple iterations in the pattern recognition step. The single-muon reconstruction efficiency is thus increased from $\simeq 85\%$ to $\simeq 98\%$ for muons from the Z boson decays with $p_{\text{T}}^{\mu} > 20$ GeV/c, reaching the efficiency level of the algorithm used for pp collisions. Background muons from cosmic rays and heavy-quark semileptonic decays are rejected by requiring a set of selection criteria on each muon track. The criteria used are based on previous studies of the performance of the muon reconstruction [19]. At least one muon detector hit is required to be included in the global-muon track fit, and segments in at least two muon detectors are required to be matched to the track in the silicon tracker. To ensure a good p_{T} measurement, at least four tracker layers with a hit are required, and the χ^2 per number of degrees of freedom of the global-muon track fit is required to be less than 10. To further reject cosmic muons and muons from decays in flight, the track is required to have a hit from at least one pixel detector layer and a transverse (longitudinal) distance of closest approach of less than 0.2

(5.0) mm from the measured primary vertex position. The most stringent selection criterion is the requirement of hits from more than one muon detector being matched to the global-muon track. The efficiency of these requirements is $\approx 98\%$ for muons from the Z boson decays, and after applying these selections, the $Z \rightarrow \mu^+\mu^-$ charge misidentification rate is less than 1% in both PbPb and pp collisions.

The electron reconstruction method uses information from the pixel and strip tracker, and the ECAL. Electrons traversing the silicon tracker can emit bremsstrahlung photons and deposit energy in the ECAL with a significant spread in the azimuthal direction. An algorithm for creating *superclusters*, which are clusters of E_T deposits from particles passing through the ECAL, is used for estimating the proper energy of photons in the heavy-ion environment, as in ref. [16]. A dedicated algorithm is used to reconstruct electrons that takes into account the bremsstrahlung emissions [28]. Track seeds in the pixel detector compatible with the superclusters are found and used to initiate the construction of particle trajectories in the inner tracker. The standard algorithms and identification criteria presented in ref. [20] are used for the pp sample, resulting in a reconstruction efficiency of about 98%. For PbPb collisions, the electron reconstruction efficiency is about 85% for $p_T^e > 20$ GeV/c electrons from the Z boson decays because the track reconstruction efficiency optimized for high-multiplicity events is lower than for pp collisions. The same electron identification variables are used in PbPb and pp collisions, with more stringent selection criteria in the latter case in order to match the ones in the $\sqrt{s} = 7$ TeV pp analyses [7, 8]. The requirements used in the selection process that have been found to be the most effective in reducing the background (see ref. [20] for definition of the variables) are: the energy-momentum combination between the supercluster and the track, the variables measuring the η and ϕ spatial matching between the track and the supercluster, the supercluster shower shape width, the hadronic leakage (the ratio of energy deposited in the HCAL and ECAL), and a transverse distance of closest approach from the measured primary vertex. These selection criteria reduce the single-electron efficiency by about 10% (5%) in PbPb (pp) collisions. After applying these criteria, the $Z \rightarrow e^+e^-$ charge misidentification rate for PbPb (pp) is less than 8% (4%), and is described well by a prediction of the combinatorial background based on same-charge pairs.

5 Signal extraction, corrections, and systematic uncertainties

5.1 Signal extraction

The Z boson candidates in PbPb and pp collisions are selected by requiring opposite-charge lepton pairs and then choosing those in the 60–120 GeV/ c^2 invariant mass region, where both leptons fulfill the acceptance and quality requirements. The acceptance requirements for both muons in PbPb and pp analyses are $p_T^\mu > 20$ GeV/c, to suppress muons from background processes, e.g. punch-through hadrons [19], and $|\eta^\mu| < 2.4$ given by the acceptance of the muon detectors. Both electrons are required to have $p_T^e > 20$ GeV/c to suppress electrons from background processes, and $|\eta^e| < 1.44$ to restrict them to be within the EB, to take advantage of a higher electron reconstruction efficiency and a better resolution in this region. In both channels, the dileptons are chosen to be in the experimentally visible

region in rapidity. The dimuon system rapidity is limited to $|y| < 2.0$, while the rapidity of the dielectron system is limited to $|y| < 1.44$.

Figure 1 shows the dimuon and the dielectron invariant mass spectra in the 60–120 GeV/ c^2 mass range after applying acceptance and selection criteria in PbPb and pp collisions. The filled histograms are from the MC simulation described in section 5.2. In the PbPb sample (top row), 1022 dimuon events (left column) with opposite-charge pairs (OC, black solid circles) and no events with same-charge pairs (SC, black open squares) are found in the Z boson mass range. The pp sample (bottom row) has 830 OC muon pairs and 1 SC pair. In the more restricted dielectron y range (right column), 328 (388) OC pairs are found in the PbPb (pp) data sample, with 27 (17) SC pairs. The increased rate of SC pairs in the dielectron channel results from higher rates of electron misreconstruction and charge misidentification. The charge misidentification rate is estimated for electrons and results in a 1% correction for Z bosons in PbPb collisions. The SC lepton pairs provide a measurement of the combinatorial background, which is negligible (at the 0.1% level) in the muon channel and about 8% (4%) in the electron channel for PbPb (pp) data. The number of Z boson candidates is taken as the OC – SC difference. The remaining background contamination is found to be less than 1% and is calculated using a sideband fitting method described in section 5.3. These sources of background include $b\bar{b}$ and $c\bar{c}$ pairs, $Z \rightarrow \tau^+\tau^-$, and combinations of charged leptons from W-boson decays with an additional misidentified lepton in the event.

5.2 Acceptance and efficiency

In order to correct yields for the acceptance and efficiency in the PbPb analysis, the electroweak processes $Z \rightarrow \mu^+\mu^-$ and $Z \rightarrow e^+e^-$ have been simulated using the PYTHIA 6.424 [29] generator, taking into account the proton and neutron content in the Pb nuclei. The detector response to each PYTHIA signal event is simulated with GEANT4 [30] and then embedded in a realistic heavy-ion background event. These background events are produced with the HYDJET 1.8 event generator [31] and then simulated with GEANT4 as well. The HYDJET parameters are tuned to reproduce the measured particle multiplicity for different centralities. The embedding is done at the level of detector hits, and the signal and background events share the same generated vertex location. The embedded events are then processed through the trigger emulation and the full event reconstruction chain. Finally, the generated Z boson p_T distribution is reweighted according to the p_T distribution obtained using the pp $\rightarrow Z \rightarrow \mu^+\mu^-$ POWHEG [32–35] next-to-leading-order (NLO) event generator at 2.76 TeV with the CT10 PDF set [36] that gives a reasonable description of the 7 TeV measurement [8]. The distribution of the longitudinal position of the primary vertex is reweighted to match the one observed in collision data.

For the pp data sample, Z boson events are generated with the PYTHIA 6.424 generator with tune Z2* that matches the charged particle multiplicity measured by CMS at \sqrt{s} values of 0.9, 2.36, and 7 TeV [37]. The generated Z boson p_T distribution is reweighted according to the same POWHEG p_T distribution used in PbPb. These generated events are reconstructed with the same software and algorithms used for the pp collision data. The longitudinal distribution of the reconstructed primary vertex matches the one in pp data.

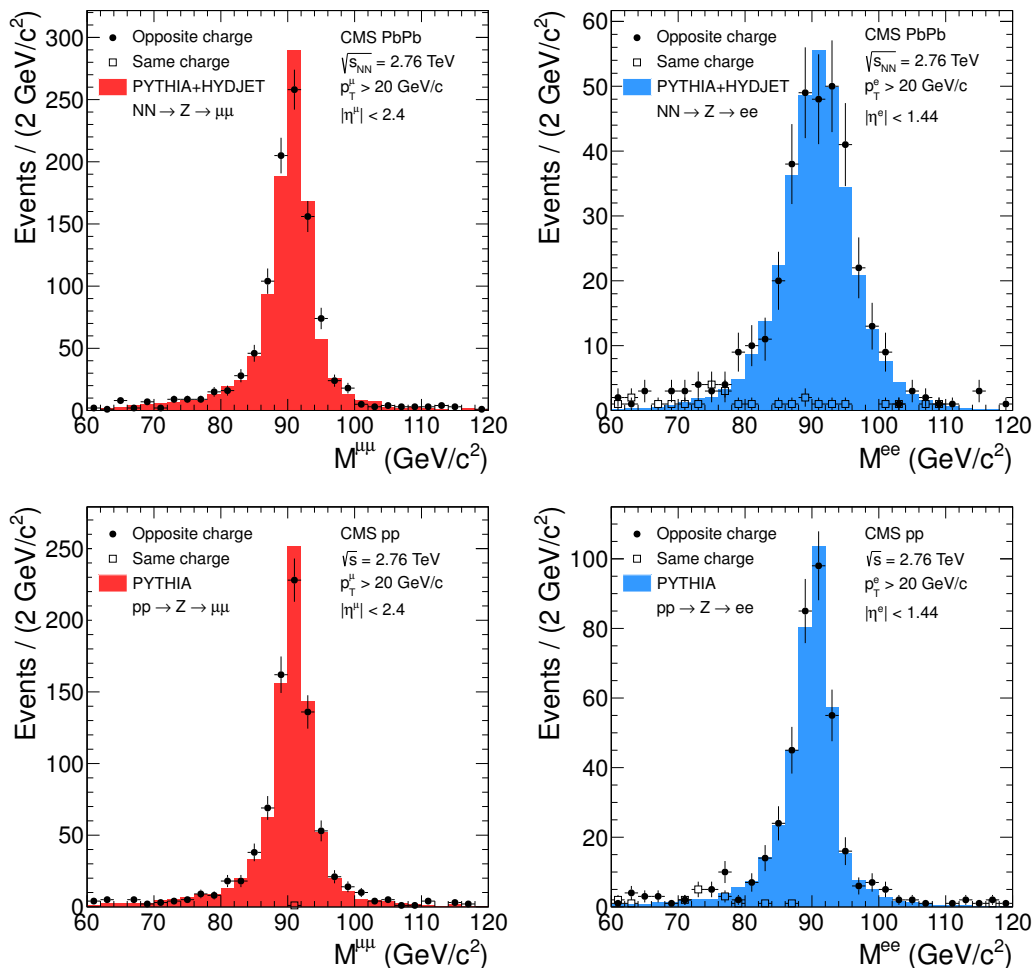


Figure 1. Dimuon invariant mass spectra for muons with $|\eta^\mu| < 2.4$ and $p_T^\mu > 20$ GeV/c in PbPb (top left) and in pp (bottom left) collisions and dielectron invariant mass spectra for electrons with $|\eta^e| < 1.44$ and $p_T^e > 20$ GeV/c in PbPb (top right) and in pp (bottom right) collisions. Full black circles represent opposite-charge lepton pair events and open black squares represent same-charge lepton pair events. Superimposed and normalized to the number of Z boson candidates in data is the MC simulation from PYTHIA $NN \rightarrow Z \rightarrow \mu^+\mu^-$ or e^+e^- , where N is a nucleon from the proper mix of protons and neutrons, embedded in HYDJET simulated events for the PbPb case, and $pp \rightarrow Z \rightarrow \mu^+\mu^-$ or e^+e^- for the pp case.

Though computed in one step, the acceptance (α) and efficiency (ε) can be split into two contributions as follows:

$$\alpha = \frac{N^Z \left(|y_Z^{\mu\mu(ee)}| < 2.0(1.44), |\eta^{\mu(e)}| < 2.4(1.44), p_T^{\mu(e)} \geq 20 \text{ GeV}/c \right)}{N^Z \left(|y_Z^{\mu\mu(ee)}| < 2.0(1.44) \right)}, \quad (5.1)$$

$$\varepsilon = \frac{N^Z \left(|y_Z^{\mu\mu(ee)}| < 2.0(1.44), |\eta^{\mu(e)}| < 2.4(1.44), p_T^{\mu(e)} \geq 20 \text{ GeV}/c, \text{ quality requirements} \right)}{N^Z \left(|y_Z^{\mu\mu(ee)}| < 2.0(1.44), |\eta^{\mu(e)}| < 2.4(1.44), p_T^{\mu(e)} \geq 20 \text{ GeV}/c \right)}, \quad (5.2)$$

where $N^Z(\dots)$ is the number of Z bosons satisfying the restrictions listed in the parentheses, and $y_Z^{\mu\mu(ee)}$ is the rapidity of the dimuon (dielectron) system. The ε factor reflects the reconstruction, trigger and selection efficiency of Z boson candidates. The corrections are calculated for each Z boson rapidity, p_T , or event centrality bin and the corresponding selection is applied to both the numerator and denominator.

For the Z boson p_T distributions, because of the rapidly falling p_T spectrum and the finite momentum resolution of the detector, an unfolding technique based on the inversion of a response matrix created from large simulation samples is first applied to data, similar to the one used in ref. [8], before applying the acceptance and efficiency correction based on the generated quantities. The p_T resolution of the Z in the dimuon (dielectron) channel varies from 7% (22%) at low Z p_T to 2.5% (2.5%) at high Z p_T . Due to the correlations between neighboring bins, the variance in the statistical uncertainties increases, which is taken into account in the quoted statistical uncertainties. Using unfolding in rapidity is not needed as the shape of the y spectrum is relatively flat.

For the Z boson rapidity distributions, the efficiency corrections are done such that the denominator is the number of generated Z boson events that survive the selection on kinematic quantities and binned in the kinematic quantities of the generated Z boson. The numerator is the number of reconstructed dimuons (dielectrons) after applying the selection criteria to the dimuon (dielectron) reconstructed quantities and binning based on those reconstructed quantities. This choice folds the minimal resolution effects in y into the efficiency correction.

The overall acceptance is approximately 70 (50)% in the muon (electron) rapidity ranges, and the overall detection efficiency is approximately 85 (55)% in PbPb and 90 (80)% in pp collisions.

5.3 Systematic uncertainties

The total systematic uncertainty in the Z boson yield in PbPb collisions is estimated by adding in quadrature the different contributions. The uncertainty on the combined trigger, reconstruction and selection efficiency is 1.8% (7.4%) for the dimuon (dielectron) channel. This estimate is based on the *tag-and-probe* technique for measuring single-particle reconstruction, identification, and trigger efficiencies, which is done in a way similar to the method described in ref. [38] and is dominated by the statistical uncertainty in the data.

Source	$Z \rightarrow \mu^+\mu^-$		$Z \rightarrow e^+e^-$	
	PbPb	pp	PbPb	pp
Combined efficiency	1.8%	1.9%	7.4%	7.7%
Acceptance	0.7%	0.7%	0.7%	0.7%
Background	0.5%	0.1%	2.0%	1.0%
N_{MB}	3.0%	–	3.0%	–
T_{AA} (N_{MB} included)	6.2%	–	6.2%	–
Integrated luminosity (L_{int})	–	3.7%	–	3.7%
Overall (without T_{AA} or L_{int})	3.6%	2.0%	8.3%	7.8%
Overall	6.5%	4.2%	9.9%	8.6%

Table 2. Summary of systematic uncertainties in the $Z \rightarrow \mu^+\mu^-$ and e^+e^- yields. PbPb values correspond to the full 0–100% centrality range. N_{MB} is the number of MB events corrected for the trigger efficiency.

The uncertainties coming from the acceptance corrections are less than 2%, as estimated by applying to the generated Z boson p_T and y distributions a weight that varies linearly between 0.7 and 1.3 over the ranges $p_T < 100 \text{ GeV}/c$ and $|y| < 2.0$ (1.44) for the dimuon (dielectron) channel. The p_T -dependent uncertainty arising from the resolution unfolding is less than 1%, as estimated by varying the generated Z boson p_T distribution using the same method. The energy scale of the electrons and muons relies heavily on the information from the track (in combination with the calorimeter and muon chambers), which decreases the uncertainty of the energy scale. The energy scale uncertainty is less than 1% for the final R_{AA} .

The systematic uncertainty from the remaining backgrounds from other physical sources, such as heavy-flavour semi-leptonic decays, is estimated by fitting the lower dilepton mass range for the data (with the Drell–Yan contribution subtracted) with an exponential function and extrapolating the fit to higher masses. This fit gives a conservative systematic uncertainty of 0.5 (2.0)% in the dimuon (dielectron) channel.

In pp collisions, the largest systematic uncertainty in the differential cross sections comes from the luminosity determination, which is 3.7%. The other sources of systematic uncertainties are similar to the ones described for PbPb collisions.

For the R_{AA} measurement described in section 6.3, the Z boson cross section in pp collisions is scaled by T_{AA} in order to compare with the corrected yields in PbPb collisions. The uncertainties in T_{AA} are derived by varying the Glauber model parameters and the minimum bias event selection efficiency within their uncertainties, resulting in 6.2% relative uncertainty for centrality-integrated quantities.

The systematic uncertainties for the $Z \rightarrow \mu^+\mu^-$ and e^+e^- channels for both yields in PbPb and pp collisions are summarized in table 2.

6 Results

6.1 Z boson production cross section in pp collisions

The differential $pp \rightarrow Z \rightarrow \mu^+\mu^-$ and e^+e^- cross sections as a function of p_T and y of the Z boson candidates, selected in the mass range between 60–120 GeV/ c^2 mass and within $|y| < 2.0$ (1.44) in the dimuon (dielectron) channel, are obtained from the pp collision data at $\sqrt{s} = 2.76$ TeV. These distributions are shown in figure 2. For pp collisions, the cross section is calculated by dividing the corrected yields by the calibrated integrated luminosity. Overall, the differential cross sections agree with the POWHEG theoretical predictions. Higher-order corrections to the cross sections predicted by this generator amount to 3% [39]. Typical next-to-next-to-leading-order calculations also have a 3% uncertainty in the proton PDFs and are found to agree with 7 and 8 TeV pp data, as reported in refs. [7, 9]. Therefore, the POWHEG reference has a typical uncertainty of 5% as indicated by the grey band.

6.2 Z boson yields in PbPb collisions vs. p_T , y , and centrality

The yield of Z bosons has been measured in PbPb collisions as a function of event centrality, Z boson y and p_T , and then compared to that in pp collisions simulated using POWHEG, scaled by an average nuclear overlap function (T_{AA}), as described below and discussed in ref. [25]. Simulated pp collisions from POWHEG are used in these first comparisons because of their higher statistical precision. As shown in section 6.1, the pp data are consistent with the simulations. A direct comparison of PbPb and pp data is shown in section 6.3.

The data are divided into independent ranges: 6 in event centrality, 8 (5) in y for the dimuon (dielectron) channel, and 7 in the dilepton p_T . The results are presented in figures 3 and 4. The yields of $Z \rightarrow \ell^+\ell^-$ (where ℓ is μ or e) per MB event, per unit of y (dN_{PbPb}^Z/dy), and per p_T bin ($d^2N_{PbPb}^Z/dy dp_T$) are computed using the following equations:

$$\frac{dN_{PbPb}^Z}{dy} = \frac{N_{PbPb}(Z \rightarrow \ell^+\ell^-)}{\alpha \varepsilon N_{MB} \Delta y} \quad \text{or} \quad \frac{d^2N_{PbPb}^Z}{dy dp_T} = \frac{N_{PbPb}(Z \rightarrow \ell^+\ell^-)}{\alpha \varepsilon N_{MB} \Delta y \Delta p_T}. \quad (6.1)$$

Here $N_{PbPb}(Z \rightarrow \ell^+\ell^-)$ is the number of Z boson candidates, divided into bins of p_T , y , and centrality, found in the dimuon or dielectron invariant mass range of 60–120 GeV/ c^2 ; N_{MB} is the number of corresponding MB events corrected for the trigger efficiency, namely $(1.16 \pm 0.03) \times 10^9$ events; α and ε are acceptance and efficiency corrections (see section 5.2); Δy and Δp_T are the two bin widths under consideration. When the Z boson yield is divided into centrality bins, N_{MB} is multiplied by the corresponding fraction of the MB cross section included in the bin.

Figure 3 shows the centrality dependence of the Z boson production in PbPb collisions. The dN_{PbPb}^Z/dy yields per MB event are divided by the nuclear overlap function T_{AA} . This quantity is proportional to the number of inelastic nucleon-nucleon collisions $N_{coll} = T_{AA} \times \sigma_{NN}^{inel}$, where $\sigma_{NN}^{inel} = 64 \pm 5$ mb is the inelastic nucleon-nucleon cross section. The T_{AA} uncertainties are included in the systematic uncertainties depicted as boxes around the data in figure 3. On the horizontal axis, the event centrality is translated to the average number of participants (N_{part}) as shown in table 1, using the same Glauber model.

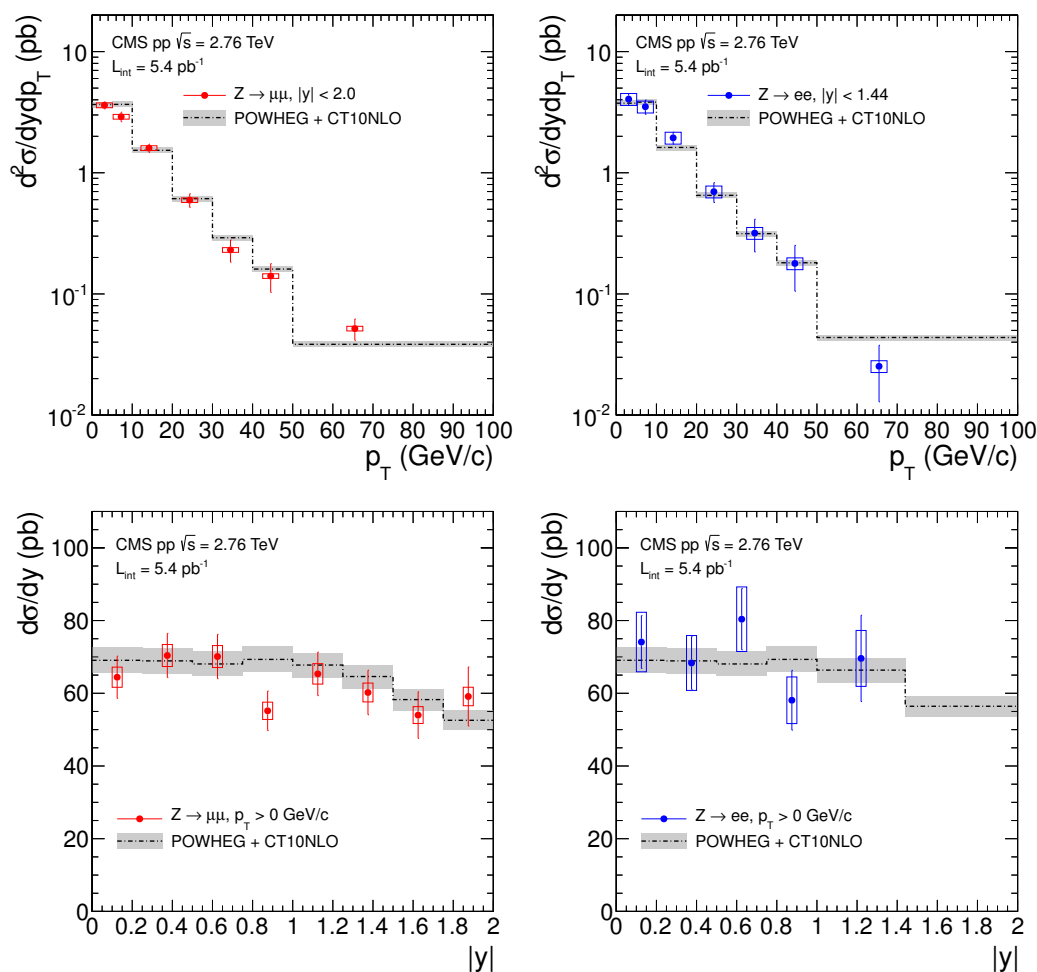


Figure 2. The measured Z boson production cross section in pp collisions as a function of the Z boson p_T (top) and y (bottom) for the dimuon (left) and the dielectron (right) decay channels. Results are compared with $pp \rightarrow Z \rightarrow \ell^+\ell^-$ POWHEG predictions. Vertical lines (boxes) correspond to statistical (systematic) uncertainties. The theoretical uncertainty of 5% assumed for the POWHEG reference curve is shown by the grey band.

No strong centrality dependence is observed for the yield $dN_{\text{PbPb}}^Z/dy \times 1/T_{\text{AA}}$. The centrality-integrated value is displayed as an open square for each channel in figure 3. For comparison, the dash-dotted line on the plots shows the cross section of the $pp \rightarrow Z \rightarrow \ell^+\ell^-$ process provided by the POWHEG generator interfaced with the PYTHIA 6.424 parton-shower generator.

For the p_T dependence and y dependence of the Z boson yields, the data are integrated over centrality; therefore the POWHEG reference is multiplied by the 0-100% centrality averaged $T_{\text{AA}} = 5.67 \pm 0.32 \text{ mb}^{-1}$, as provided by the Glauber model described above. By construction, this centrality-averaged T_{AA} is equal to $A^2/\sigma_{\text{PbPb}}^{\text{inel}}$, where $A = 208$ is the Pb atomic number and $\sigma_{\text{PbPb}}^{\text{inel}} = 7.65 \pm 0.42 \text{ barns}$ is the total PbPb inelastic cross section computed from the same Glauber model.

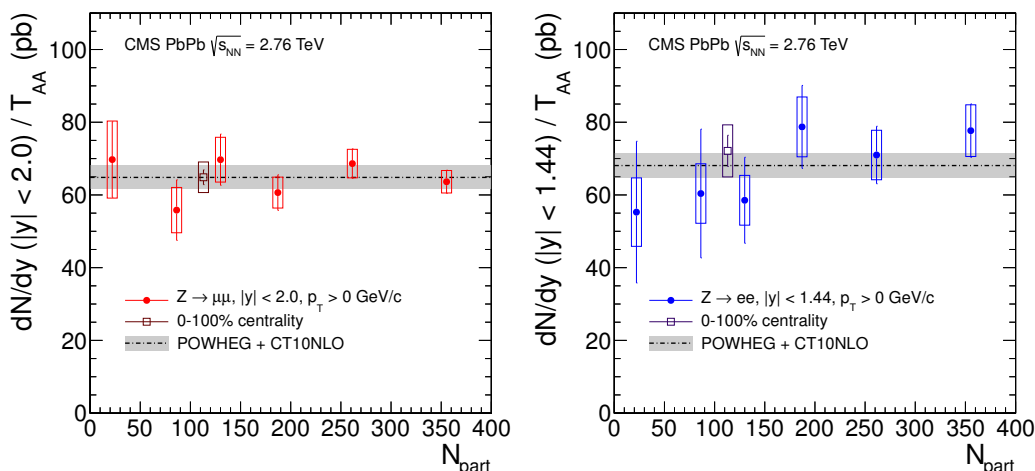


Figure 3. Event centrality dependence of the $Z \rightarrow \mu^+\mu^-$ (left) and $Z \rightarrow e^+e^-$ (right) yields per MB event in PbPb collisions, divided by the expected average nuclear overlap function, T_{AA} , which is directly comparable to the $pp \rightarrow Z \rightarrow \ell^+\ell^-$ cross section predicted by the POWHEG generator displayed as a black dash-dotted line. On the horizontal axis, event centrality is depicted as the average number of participating nucleons, N_{part} (see table 1). Vertical lines (boxes) correspond to statistical (systematic) uncertainties. The theoretical uncertainty of 5% assumed for the POWHEG reference curve is shown by the grey band.

Figure 4 shows the distribution $d^2N_{\text{PbPb}}^Z/dy dp_T$ as a function of the dilepton p_T and the invariant yield as a function of rapidity, dN_{PbPb}^Z/dy compared to theoretical predictions, as follows. The results vs. p_T are compared to POWHEG, while the results vs. y are compared to predictions from Paukkunen and Salgado [12] which do not incorporate nuclear PDF modifications to the unbound proton/nucleon PDFs (yellow light band) and those that do (green dark band) through the nuclear PDF set EPS09 [40]. No strong deviations from these absolutely-normalized references are observed.

The Z boson yields in PbPb collisions have been compared with various theoretical predictions, including PDFs that incorporate nuclear effects. The calculated yields are found to be consistent with the results. Therefore, we deduce that Z boson production scales with the number of inelastic nucleon-nucleon collisions. Furthermore, nuclear effects such as isospin or shadowing are small compared to the statistical uncertainties, hence it is not possible to discriminate among these nuclear effects with the available data.

6.3 Nuclear modification factor

Based on PbPb and pp data at the same centre-of-mass energy, the nuclear modification factor, R_{AA} , is computed for both the dimuon and dielectron channels as a function of the Z boson p_T , y , and event centrality, as follows:

$$R_{AA} = \frac{N_{\text{PbPb}}^Z}{T_{AA} \times \sigma_{pp}^Z} \equiv \frac{N_{\text{PbPb}}^Z}{N_{\text{coll}} \times N_{pp}^Z} \quad (6.2)$$

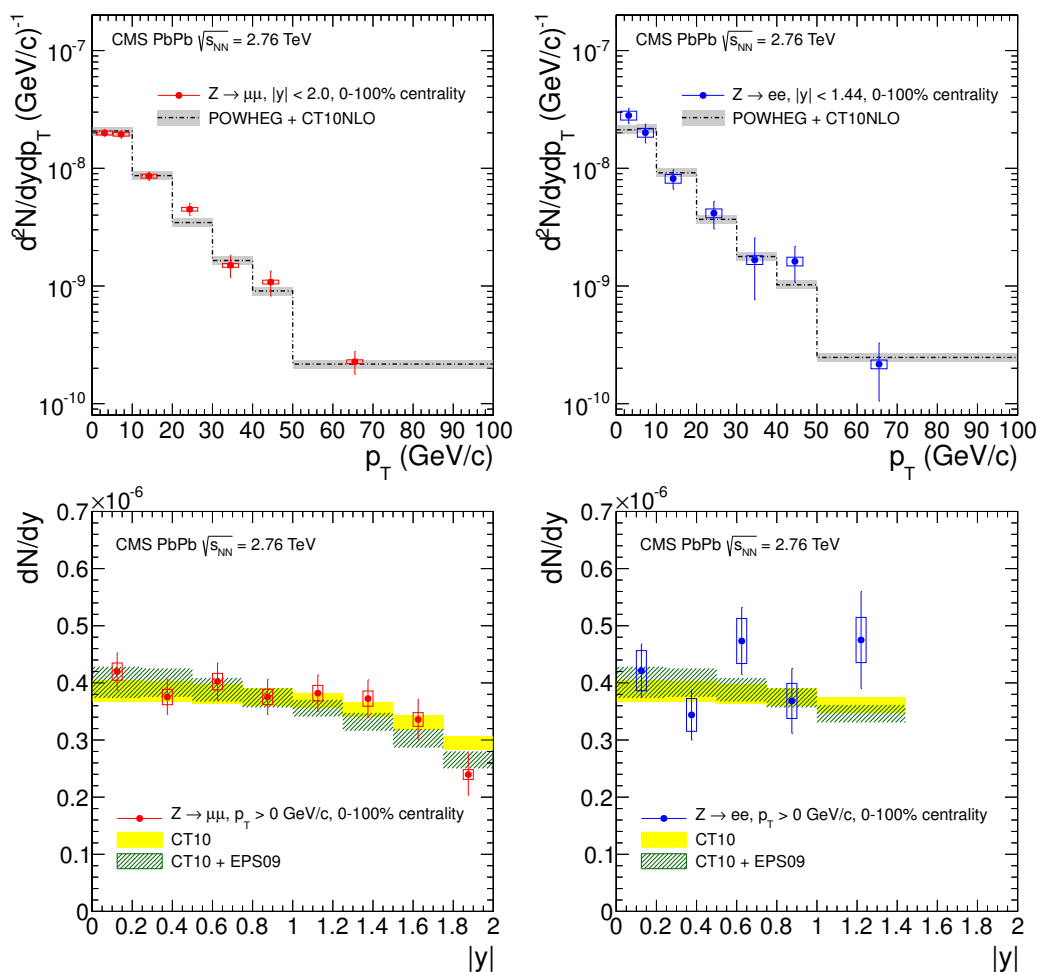


Figure 4. The measured Z boson yields per MB event in PbPb collisions as a function of the Z boson p_T (top) and y (bottom) for the dimuon (left) and the dielectron (right) decay channels. The yields are compared with $pp \rightarrow Z \rightarrow \ell^+\ell^-$ POWHEG predictions scaled by the 0–100% centrality averaged T_{AA} . The light gray bands in the results vs. p_T represent the theoretical uncertainty of 5% assumed for the POWHEG reference curve together with the uncertainty of 6.2% due to the T_{AA} scaling. The results vs. y are compared to predictions with (green dark band) and without (yellow light band) nuclear modification effects. Vertical lines (boxes) correspond to statistical (systematic) uncertainties.

where N_{PbPb}^Z (N_{pp}^Z) are the yields per MB event measured (in PbPb (pp) collisions corrected for acceptance and efficiency, σ_{pp}^Z refers to the differential cross sections measured from pp collisions, N_{coll} refers to the average number of inelastic nucleon-nucleon collisions for the appropriate centrality selection, and T_{AA} refers to the values of the nuclear overlap function as described in section 3. The R_{AA} values as a function of y , p_T and centrality are shown in figure 5 (where the points are slightly shifted along the horizontal axis for clarity: left for muons and right for electrons), and in table 3.

The information in figure 5 is similar to that shown in figures 3 and 4 but here using pp data for comparison instead of POWHEG simulations. The R_{AA} values show no dependence,

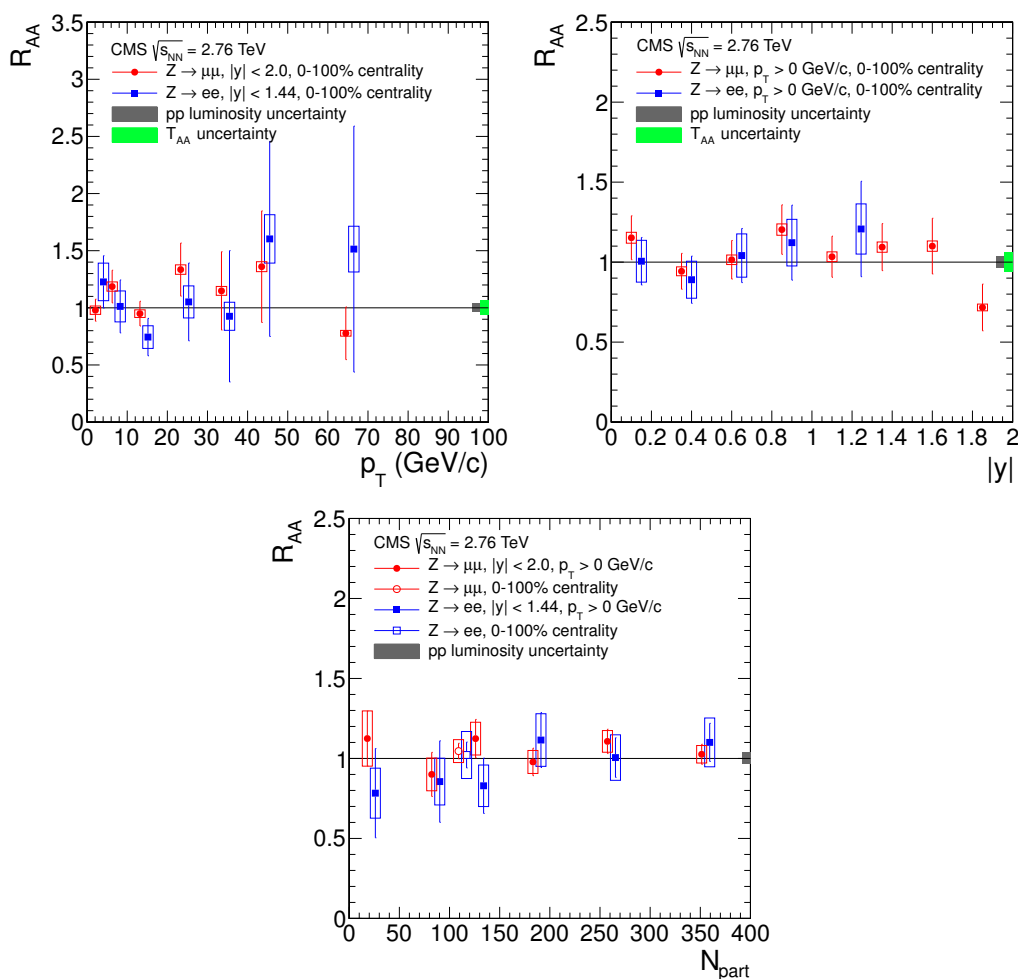


Figure 5. The R_{AA} distribution for the $Z \rightarrow e^+e^-$ (blue squares) and $Z \rightarrow \mu^+\mu^-$ (red circles) events as a function of the Z boson p_T (left), y (right), and N_{part} (bottom). For N_{part} , open points at $N_{part} \sim 110$ represent the centrality-integrated R_{AA} . Points are shifted along the horizontal axis for clarity. The horizontal line at $R_{AA} = 1$ is drawn as a reference. Vertical lines (boxes) correspond to statistical (systematic) uncertainties. The grey bar at $R_{AA} = 1$ corresponds to uncertainty in pp luminosity and the green bar corresponds to uncertainty in T_{AA} .

and hence no variation in nuclear effects, as a function of p_T , y , or centrality in both the muon and electron channels in the kinematic range studied and within the current uncertainties.

6.4 Combined results for the two decay channels

According to lepton universality and given the large mass, the Z boson is expected to decay into the dimuon and dielectron channels with branching ratios within 1% of each other. Also, neither muons nor electrons are expected to interact strongly with the medium formed in the collision. The two channels can therefore be checked against each other, and used to measure the combined $Z \rightarrow \ell^+\ell^-$ yields and R_{AA} , where $Z \rightarrow \ell^+\ell^-$ refers to the Z

R_{AA}			
$ y $	$Z \rightarrow \mu^+\mu^-$	$Z \rightarrow e^+e^-$	$Z \rightarrow \ell^+\ell^-$
[0.00, 0.25]	$1.17 \pm 0.14 \pm 0.09$	$1.01 \pm 0.15 \pm 0.15$	$1.13 \pm 0.11 \pm 0.09$
[0.25, 0.50]	$0.96 \pm 0.11 \pm 0.07$	$0.89 \pm 0.15 \pm 0.13$	$0.96 \pm 0.09 \pm 0.08$
[0.50, 0.75]	$1.03 \pm 0.12 \pm 0.08$	$1.04 \pm 0.17 \pm 0.15$	$1.04 \pm 0.10 \pm 0.09$
[0.75, 1.00]	$1.22 \pm 0.16 \pm 0.10$	$1.12 \pm 0.23 \pm 0.17$	$1.22 \pm 0.13 \pm 0.10$
[1.00, 1.25]	$1.05 \pm 0.13 \pm 0.08$	–	–
[1.25, 1.50]	$1.11 \pm 0.15 \pm 0.09$	–	–
[1.00, 1.44]	–	$1.21 \pm 0.30 \pm 0.18$	$1.14 \pm 0.10 \pm 0.09$
[1.50, 1.75]	$1.12 \pm 0.18 \pm 0.09$	–	$1.12 \pm 0.18 \pm 0.09$
[1.75, 2.00]	$0.73 \pm 0.15 \pm 0.06$	–	$0.73 \pm 0.15 \pm 0.06$
$p_T(\text{GeV}/c)$			
[0, 5]	$0.99 \pm 0.09 \pm 0.08$	$1.23 \pm 0.23 \pm 0.19$	$0.99 \pm 0.09 \pm 0.08$
[5, 10]	$1.20 \pm 0.13 \pm 0.10$	$1.01 \pm 0.23 \pm 0.15$	$1.29 \pm 0.14 \pm 0.11$
[10, 20]	$0.96 \pm 0.10 \pm 0.08$	$0.74 \pm 0.16 \pm 0.11$	$0.93 \pm 0.10 \pm 0.08$
[20, 30]	$1.36 \pm 0.22 \pm 0.11$	$1.05 \pm 0.34 \pm 0.16$	$1.27 \pm 0.20 \pm 0.11$
[30, 40]	$1.17 \pm 0.32 \pm 0.09$	$0.93 \pm 0.57 \pm 0.14$	$1.18 \pm 0.31 \pm 0.10$
[40, 50]	$1.38 \pm 0.47 \pm 0.11$	$1.60 \pm 0.85 \pm 0.24$	$1.28 \pm 0.40 \pm 0.11$
[50, 100]	$0.79 \pm 0.23 \pm 0.06$	$1.51 \pm 1.08 \pm 0.23$	$0.89 \pm 0.28 \pm 0.07$
Centrality			
[0, 10]%	$1.04 \pm 0.06 \pm 0.07$	$1.10 \pm 0.12 \pm 0.16$	$1.10 \pm 0.06 \pm 0.07$
[10, 20]%	$1.12 \pm 0.08 \pm 0.08$	$1.01 \pm 0.12 \pm 0.15$	$1.14 \pm 0.08 \pm 0.08$
[20, 30]%	$0.99 \pm 0.09 \pm 0.08$	$1.12 \pm 0.17 \pm 0.17$	$1.12 \pm 0.09 \pm 0.09$
[30, 40]%	$1.14 \pm 0.12 \pm 0.11$	$0.83 \pm 0.17 \pm 0.13$	$1.06 \pm 0.11 \pm 0.10$
[40, 50]%	$0.91 \pm 0.14 \pm 0.11$	$0.86 \pm 0.25 \pm 0.15$	$0.94 \pm 0.14 \pm 0.11$
[50, 100]%	$1.14 \pm 0.17 \pm 0.18$	$0.78 \pm 0.28 \pm 0.16$	$1.17 \pm 0.17 \pm 0.18$
[0, 100]%	$1.06 \pm 0.05 \pm 0.08$	$1.02 \pm 0.08 \pm 0.15$	$1.10 \pm 0.05 \pm 0.09$

Table 3. Nuclear modification factor (R_{AA}) for the $Z \rightarrow \ell^+\ell^-$ process as a function of rapidity, p_T , and event centrality. The rapidity integrated values are shown for $|y| < 2.0$ for the muon channel and for $|y| < 1.44$ in case of the electron channel and for the combined channel. The first uncertainty is statistical and the second one is systematic.

boson decaying into either the dimuon or dielectron channel. Given the uncertainties in the measurements, in the region of overlap, the datasets are in agreement. The combination is then done following the best linear unbiased estimate technique, as described in ref. [41].

The combined yields per MB event for PbPb collisions and the combined cross sections for pp collisions are shown in figures 6 and 7, respectively. The dimuon and dielectron measurements share the kinematic region of $|y| < 1.44$. The dependence on p_T and N_{part} of the Z boson yield and R_{AA} measurements in the combination of the two channels are therefore restricted to $|y| < 1.44$. The dependence on $|y|$ is shown with the combined measurements for $|y| < 1.44$, extended with the dimuon measurements for the $1.5 < |y| < 2.0$ range.

The results as a function of p_T , y , and centrality are compared with predictions from the POWHEG generator; this comparison shows that the measurements agree with the theoretical calculations within the combined statistical and systematic uncertainties. The current precision of the measurements does not allow to distinguish between the unbound proton PDF sets and the modified nuclear PDF sets.

To calculate the combined R_{AA} , the combined dilepton yields in PbPb and pp data are obtained and then the R_{AA} ratio is calculated based on those values. The combined R_{AA} values are given in table 3 and in figure 8. The R_{AA} for the combination of the two channels shows no dependence and no variation in nuclear effects as a function of p_T , y , or centrality. This demonstrates that within uncertainties, Z boson production is not modified in PbPb collisions compared with pp collisions scaled by the number of inelastic nucleon-nucleon collisions.

7 Summary

The yields of Z bosons have been measured as a function of p_T , y , and centrality, in both the dimuon and dielectron channels for PbPb collisions at $\sqrt{s_{NN}}$ of 2.76 TeV with an integrated luminosity of approximately $166 \mu\text{b}^{-1}$. The $Z \rightarrow \mu^+\mu^-$ and $Z \rightarrow e^+e^-$ cross sections have been measured in pp collisions at the same collision energy with an integrated luminosity of 5.4pb^{-1} . Within the combined statistical and systematic uncertainties, no centrality dependence is observed once the yields are normalized by the number of inelastic nucleon-nucleon collisions. When integrated over centrality, the Z boson y and p_T distributions are found to be consistent between the PbPb and pp data and also to agree with theoretical predictions. The centrality-integrated R_{AA} is found to be 1.06 ± 0.05 (stat) ± 0.08 (syst) in the dimuon channel and 1.02 ± 0.08 (stat) ± 0.15 (syst) in the dielectron channel. No significant nuclear modifications are found as a function of p_T , y , or centrality in either the dimuon or dielectron channels over the entire kinematic range studied.

Acknowledgments

We congratulate our colleagues in the CERN accelerator departments for the excellent performance of the LHC and thank the technical and administrative staffs at CERN and at other CMS institutes for their contributions to the success of the CMS effort. In addition, we gratefully acknowledge the computing centres and personnel of the Worldwide

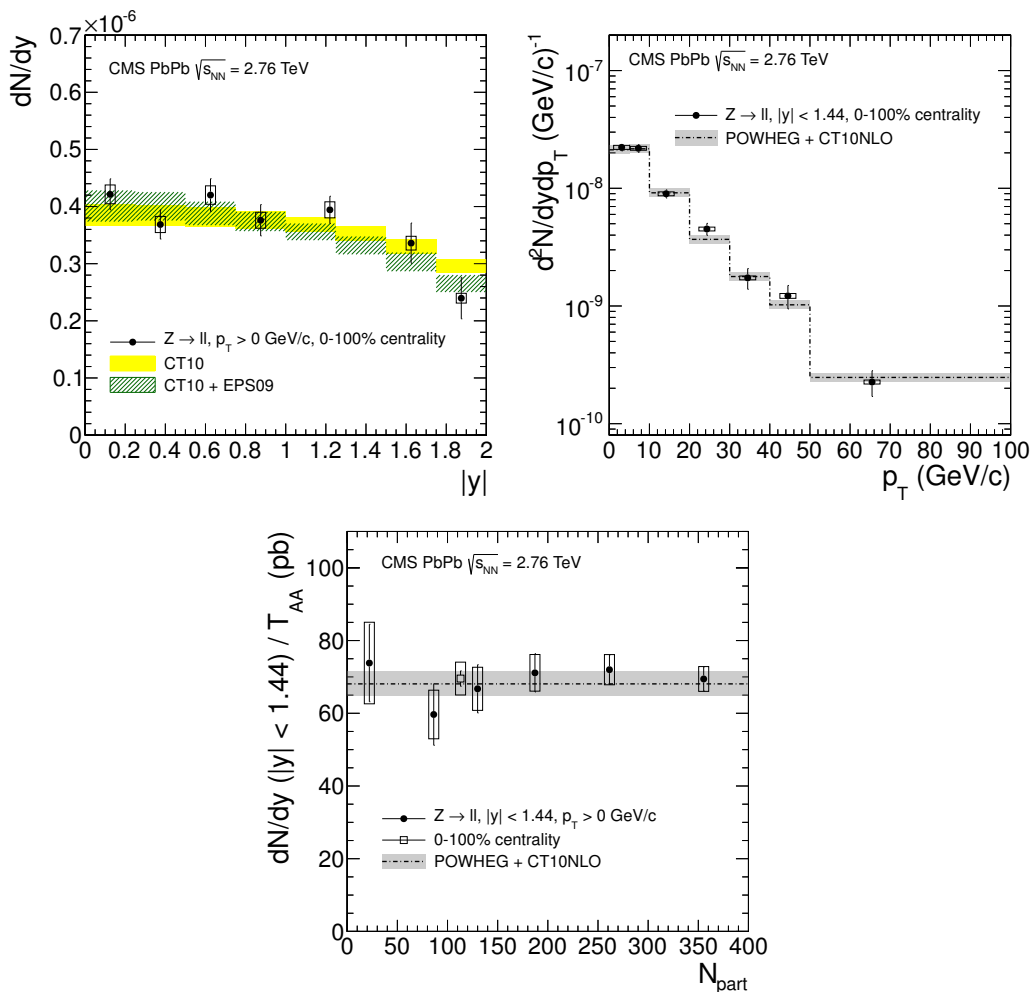


Figure 6. The measured $Z \rightarrow \ell^+\ell^-$ yields per MB event in PbPb collisions, shown for the combined leptonic channel as a function of the Z boson y (top left), p_T (top right), and N_{part} (bottom). For the y dependence, the measurements from dimuons and dielectrons are combined for $|y| < 1.44$, and the dimuon measurements alone are shown for $1.5 < |y| < 2.0$. The yields are compared with $pp \rightarrow Z \rightarrow \ell^+\ell^-$ POWHEG predictions scaled by the 0–100% centrality averaged T_{AA} . The light gray bands represent the theoretical uncertainty of 5% assumed for the POWHEG reference curve together with the uncertainty of 6.2% due to the T_{AA} scaling. The results vs. y are compared to predictions with (green dark band) and without (yellow light band) nuclear modification effects. Vertical lines (boxes) correspond to statistical (systematic) uncertainties.

LHC Computing Grid for delivering so effectively the computing infrastructure essential to our analyses. Finally, we acknowledge the enduring support for the construction and operation of the LHC and the CMS detector provided by the following funding agencies: BMFW and FWF (Austria); FNRS and FWO (Belgium); CNPq, CAPES, FAPERJ, and FAPESP (Brazil); MES (Bulgaria); CERN; CAS, MoST, and NSFC (China); COLCIENCIAS (Colombia); MSES and CSF (Croatia); RPF (Cyprus); MoER, ERC IUT and ERDF (Estonia); Academy of Finland, MEC, and HIP (Finland); CEA and CNRS/IN2P3

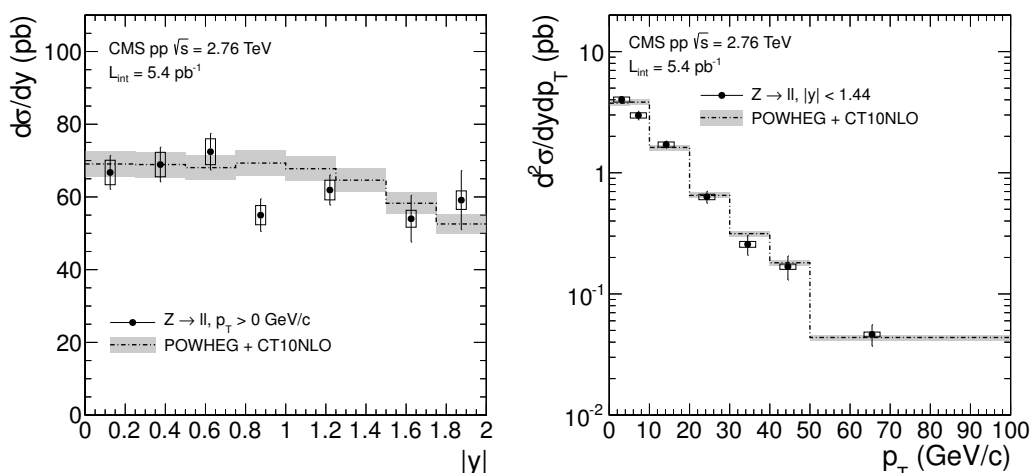


Figure 7. The measured $Z \rightarrow \ell^+ \ell^-$ cross section in pp collisions, shown for the combined leptonic channel as a function of the Z boson y (left) and p_T (right). For the y dependence, the measurements from dimuons and dielectrons are combined for $|y| < 1.44$, and the dimuon measurements alone are shown for $1.5 < |y| < 2.0$. Results are compared with pp $\rightarrow Z \rightarrow \ell^+ \ell^-$ POWHEG predictions. Vertical lines (boxes) correspond to statistical (systematic) uncertainties. The theoretical uncertainty of 5% assumed for the POWHEG reference curve is shown by the grey band.

(France); BMBF, DFG, and HGF (Germany); GSRT (Greece); OTKA and NIH (Hungary); DAE and DST (India); IPM (Iran); SFI (Ireland); INFN (Italy); NRF and WCU (Republic of Korea); LAS (Lithuania); MOE and UM (Malaysia); CINVESTAV, CONACYT, SEP, and UASLP-FAI (Mexico); MBIE (New Zealand); PAEC (Pakistan); MSHE and NSC (Poland); FCT (Portugal); JINR (Dubna); MON, RosAtom, RAS and RFBR (Russia); MESTD (Serbia); SEIDI and CPAN (Spain); Swiss Funding Agencies (Switzerland); MST (Taipei); ThEPCenter, IPST, STAR and NSTDA (Thailand); TUBITAK and TAEK (Turkey); NASU and SFFR (Ukraine); STFC (United Kingdom); DOE and NSF (USA).

Individuals have received support from the Marie-Curie programme and the European Research Council and EPLANET (European Union); the Leventis Foundation; the A. P. Sloan Foundation; the Alexander von Humboldt Foundation; the Belgian Federal Science Policy Office; the Fonds pour la Formation à la Recherche dans l'Industrie et dans l'Agriculture (FRIA-Belgium); the Agentschap voor Innovatie door Wetenschap en Technologie (IWT-Belgium); the Ministry of Education, Youth and Sports (MEYS) of the Czech Republic; the Council of Science and Industrial Research, India; the HOMING PLUS programme of Foundation for Polish Science, cofinanced from European Union, Regional Development Fund; the Compagnia di San Paolo (Torino); the Consorzio per la Fisica (Trieste); MIUR project 20108T4XTM (Italy); the Thalys and Aristeia programmes cofinanced by EU-ESF and the Greek NSRF; and the National Priorities Research Program by Qatar National Research Fund.

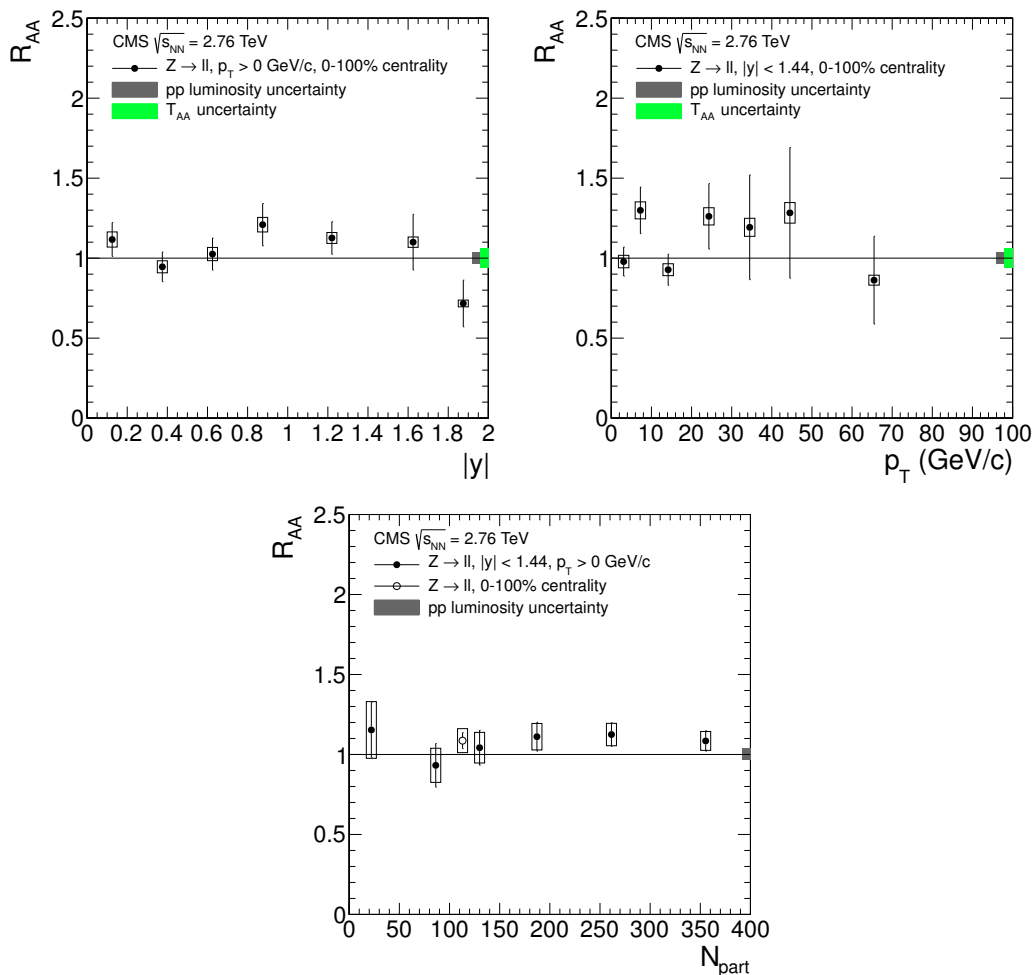


Figure 8. The Z boson R_{AA} values for the combination of the dimuon and dielectron channel, as a function of y (top left), p_T (top right), and N_{part} (bottom). The horizontal line at $R_{AA} = 1$ is drawn as a reference. Vertical lines (boxes) correspond to statistical (systematic) uncertainties. Grey light bar at $R_{AA} = 1$ corresponds to uncertainty in pp luminosity and green dark bar corresponds to uncertainty of T_{AA} .

Open Access. This article is distributed under the terms of the Creative Commons Attribution License ([CC-BY 4.0](https://creativecommons.org/licenses/by/4.0/)), which permits any use, distribution and reproduction in any medium, provided the original author(s) and source are credited.

References

- [1] UA1 collaboration, G. Arnison et al., *Experimental observation of lepton pairs of invariant mass around $95 \text{ GeV}/c^2$ at the CERN SPS collider*, *Phys. Lett. B* **126** (1983) 398 [[INSPIRE](#)].
- [2] UA2 collaboration, P. Bagnaia et al., *Evidence for $Z^0 \rightarrow e^+e^-$ at the CERN $\bar{p}p$ collider*, *Phys. Lett. B* **129** (1983) 130 [[INSPIRE](#)].
- [3] ALEPH, DELPHI, L3, OPAL and LEP ELECTROWEAK collaborations, *Electroweak Measurements in Electron-Positron Collisions at W-Boson-Pair Energies at LEP*, *Phys. Rept.* **532** (2013) 119 [[arXiv:1302.3415](#)] [[INSPIRE](#)].
- [4] ALEPH, DELPHI, L3, OPAL, SLD, LEP ELECTROWEAK WORKING GROUP, SLD ELECTROWEAK GROUP and SLD HEAVY FLAVOUR GROUP collaborations, *Precision electroweak measurements on the Z resonance*, *Phys. Rept.* **427** (2006) 257 [[hep-ex/0509008](#)] [[INSPIRE](#)].
- [5] CDF collaboration, D. Acosta et al., *First measurements of inclusive W and Z cross sections from Run II of the Tevatron collider*, *Phys. Rev. Lett.* **94** (2005) 091803 [[hep-ex/0406078](#)] [[INSPIRE](#)].
- [6] D0 collaboration, S. Abachi et al., *W and Z boson production in $p\bar{p}$ collisions at $\sqrt{s} = 1.8 \text{ TeV}$* , *Phys. Rev. Lett.* **75** (1995) 1456 [[hep-ex/9505013](#)] [[INSPIRE](#)].
- [7] CMS collaboration, *Measurement of the inclusive W and Z production cross sections in pp collisions at $\sqrt{s} = 7 \text{ TeV}$* , *JHEP* **10** (2011) 132 [[arXiv:1107.4789](#)] [[INSPIRE](#)].
- [8] CMS collaboration, *Measurement of the rapidity and transverse momentum distributions of Z bosons in pp collisions at $\sqrt{s} = 7 \text{ TeV}$* , *Phys. Rev. D* **85** (2012) 032002 [[arXiv:1110.4973](#)] [[INSPIRE](#)].
- [9] CMS collaboration, *Measurement of inclusive W and Z boson production cross sections in pp collisions at $\sqrt{s} = 8 \text{ TeV}$* , *Phys. Rev. Lett.* **112** (2014) 191802 [[arXiv:1402.0923](#)] [[INSPIRE](#)].
- [10] ATLAS collaboration, *Measurement of the inclusive W^\pm and Z/γ cross sections in the electron and muon decay channels in pp collisions at $\sqrt{s} = 7 \text{ TeV}$ with the ATLAS detector*, *Phys. Rev. D* **85** (2012) 072004 [[arXiv:1109.5141](#)] [[INSPIRE](#)].
- [11] V. Kartvelishvili, R. Kvatadze and R. Shanidze, *On Z and Z + jet production in heavy ion collisions*, *Phys. Lett. B* **356** (1995) 589 [[hep-ph/9505418](#)] [[INSPIRE](#)].
- [12] H. Paukkunen and C.A. Salgado, *Constraints for the nuclear parton distributions from Z and W production at the LHC*, *JHEP* **03** (2011) 071 [[arXiv:1010.5392](#)] [[INSPIRE](#)].
- [13] R.B. Neufeld, I. Vitev and B.-W. Zhang, *A possible determination of the quark radiation length in cold nuclear matter*, *Phys. Lett. B* **704** (2011) 590 [[arXiv:1010.3708](#)] [[INSPIRE](#)].
- [14] CMS collaboration, *Study of Z boson production in PbPb collisions at $\sqrt{s_{NN}} = 2.76 \text{ TeV}$* , *Phys. Rev. Lett.* **106** (2011) 212301 [[arXiv:1102.5435](#)] [[INSPIRE](#)].
- [15] CMS collaboration, *Study of W boson production in PbPb and pp collisions at $\sqrt{s_{NN}} = 2.76 \text{ TeV}$* , *Phys. Lett. B* **715** (2012) 66 [[arXiv:1205.6334](#)] [[INSPIRE](#)].

- [16] CMS collaboration, *Measurement of isolated photon production in pp and PbPb collisions at $\sqrt{s_{NN}} = 2.76$ TeV*, *Phys. Lett. B* **710** (2012) 256 [[arXiv:1201.3093](#)] [[INSPIRE](#)].
- [17] ATLAS collaboration, *Measurement of Z boson Production in Pb+Pb Collisions at $\sqrt{s_{NN}} = 2.76$ TeV with the ATLAS Detector*, *Phys. Rev. Lett.* **110** (2013) 022301 [[arXiv:1210.6486](#)] [[INSPIRE](#)].
- [18] CMS collaboration, *The CMS experiment at the CERN LHC, 2008* *JINST* **3** S08004 [[INSPIRE](#)].
- [19] CMS collaboration, *Performance of CMS muon reconstruction in pp collision events at $\sqrt{s} = 7$ TeV*, 2012 *JINST* **7** P10002 [[arXiv:1206.4071](#)] [[INSPIRE](#)].
- [20] CMS collaboration, *Energy calibration and resolution of the CMS electromagnetic calorimeter in pp collisions at $\sqrt{s} = 7$ TeV*, 2013 *JINST* **8** P09009 [[arXiv:1306.2016](#)] [[INSPIRE](#)].
- [21] CMS collaboration, *Observation and studies of jet quenching in PbPb collisions at $\sqrt{s_{NN}} = 2.76$ TeV*, *Phys. Rev. C* **84** (2011) 024906 [[arXiv:1102.1957](#)] [[INSPIRE](#)].
- [22] CMS collaboration, *Luminosity Calibration for the 2013 Proton-Lead and Proton-Proton Data Taking*, *CMS-PAS-LUM-13-002* (2013).
- [23] CMS collaboration, *CMS technical design report, volume II: Physics performance*, *J. Phys. G* **34** (2007) 995 [[INSPIRE](#)].
- [24] CMS collaboration, *Measurement of the differential cross section for isolated prompt photon production in pp collisions at 7 TeV*, *Phys. Rev. D* **84** (2011) 052011 [[arXiv:1108.2044](#)] [[INSPIRE](#)].
- [25] M.L. Miller, K. Reygers, S.J. Sanders and P. Steinberg, *Glauber modeling in high energy nuclear collisions*, *Ann. Rev. Nucl. Part. Sci.* **57** (2007) 205 [[nucl-ex/0701025](#)] [[INSPIRE](#)].
- [26] B. Alver, M. Baker, C. Loizides and P. Steinberg, *The PHOBOS Glauber Monte Carlo*, [arXiv:0805.4411](#) [[INSPIRE](#)].
- [27] PARTICLE DATA GROUP, J. Beringer et al., *Review of Particle Physics (RPP)*, *Phys. Rev. D* **86** (2012) 010001 [[INSPIRE](#)].
- [28] W. Adam, R. Fruhwirth, A. Strandlie and T. Todorov, *Reconstruction of electrons with the Gaussian sum filter in the CMS tracker at LHC*, *eConf C* **0303241** (2003) TULT009 [[physics/0306087](#)] [[INSPIRE](#)].
- [29] T. Sjöstrand, S. Mrenna and P.Z. Skands, *PYTHIA 6.4 physics and manual*, *JHEP* **05** (2006) 026 [[hep-ph/0603175](#)] [[INSPIRE](#)].
- [30] GEANT4 collaboration, S. Agostinelli et al., *GEANT4 — a simulation toolkit*, *Nucl. Instrum. Meth. A* **506** (2003) 250 [[INSPIRE](#)].
- [31] I.P. Lokhtin and A.M. Snigirev, *A model of jet quenching in ultrarelativistic heavy ion collisions and high- p_T hadron spectra at RHIC*, *Eur. Phys. J. C* **45** (2006) 211 [[hep-ph/0506189](#)] [[INSPIRE](#)].
- [32] P. Nason, *A new method for combining NLO QCD with shower Monte Carlo algorithms*, *JHEP* **11** (2004) 040 [[hep-ph/0409146](#)] [[INSPIRE](#)].
- [33] S. Frixione, P. Nason and C. Oleari, *Matching NLO QCD computations with Parton Shower simulations: the POWHEG method*, *JHEP* **11** (2007) 070 [[arXiv:0709.2092](#)] [[INSPIRE](#)].

- [34] S. Alioli, P. Nason, C. Oleari and E. Re, *NLO vector-boson production matched with shower in POWHEG*, *JHEP* **07** (2008) 060 [[arXiv:0805.4802](#)] [[INSPIRE](#)].
- [35] S. Alioli, P. Nason, C. Oleari and E. Re, *A general framework for implementing NLO calculations in shower Monte Carlo programs: the POWHEG BOX*, *JHEP* **06** (2010) 043 [[arXiv:1002.2581](#)] [[INSPIRE](#)].
- [36] H.-L. Lai et al., *New parton distributions for collider physics*, *Phys. Rev. D* **82** (2010) 074024 [[arXiv:1007.2241](#)] [[INSPIRE](#)].
- [37] CMS collaboration, *Study of the underlying event at forward rapidity in pp collisions at $\sqrt{s} = 0.9, 2.76$ and 7 TeV*, *JHEP* **04** (2013) 072 [[arXiv:1302.2394](#)] [[INSPIRE](#)].
- [38] CMS collaboration, *Suppression of non-prompt J/ψ , prompt J/ψ and $Y(1S)$ in PbPb collisions at $\sqrt{s_{NN}} = 2.76$ TeV*, *JHEP* **05** (2012) 063 [[arXiv:1201.5069](#)] [[INSPIRE](#)].
- [39] S. Catani, L. Cieri, G. Ferrera, D. de Florian and M. Grazzini, *Vector boson production at hadron colliders: a fully exclusive QCD calculation at NNLO*, *Phys. Rev. Lett.* **103** (2009) 082001 [[arXiv:0903.2120](#)] [[INSPIRE](#)].
- [40] K.J. Eskola, H. Paukkunen and C.A. Salgado, *EPS09: A new generation of NLO and LO nuclear parton distribution functions*, *JHEP* **04** (2009) 065 [[arXiv:0902.4154](#)] [[INSPIRE](#)].
- [41] L. Lyons, D. Gibaut and P. Clifford, *How to combine correlated estimates of a single physical quantity*, *Nucl. Instrum. Meth. A* **270** (1988) 110 [[INSPIRE](#)].

The CMS collaboration

Yerevan Physics Institute, Yerevan, Armenia

S. Chatrchyan, V. Khachatryan, A.M. Sirunyan

Institut für Hochenergiephysik der OeAW, Wien, Austria

W. Adam, T. Bergauer, M. Dragicevic, J. Erö, C. Fabjan¹, M. Friedl, R. Frühwirth¹, V.M. Ghete, C. Hartl, N. Hörmann, J. Hrubec, M. Jeitler¹, W. Kiesenhofer, V. Knünz, M. Krammer¹, I. Krätschmer, D. Liko, I. Mikulec, D. Rabady², B. Rahbaran, H. Rohringer, R. Schöfbeck, J. Strauss, A. Taurok, W. Treberer-Treberspurg, W. Waltenberger, C.-E. Wulz¹

National Centre for Particle and High Energy Physics, Minsk, Belarus

V. Mossolov, N. Shumeiko, J. Suarez Gonzalez

Universiteit Antwerpen, Antwerpen, Belgium

S. Alderweireldt, M. Bansal, S. Bansal, T. Cornelis, E.A. De Wolf, X. Janssen, A. Knutsson, S. Luyckx, S. Ochesanu, B. Roland, R. Rougny, M. Van De Klundert, H. Van Haeevermaet, P. Van Mechelen, N. Van Remortel, A. Van Spilbeeck

Vrije Universiteit Brussel, Brussel, Belgium

F. Blekman, S. Blyweert, J. D'Hondt, N. Daci, N. Heracleous, J. Keaveney, S. Lowette, M. Maes, A. Olbrechts, Q. Python, D. Strom, S. Tavernier, W. Van Doninck, P. Van Mulders, G.P. Van Onsem, I. Villella

Université Libre de Bruxelles, Bruxelles, Belgium

C. Caillol, B. Clerbaux, G. De Lentdecker, D. Dobur, L. Favart, A.P.R. Gay, A. Grebenyuk, A. Léonard, A. Mohammadi, L. Perniè², T. Reis, T. Seva, L. Thomas, C. Vander Velde, P. Vanlaer, J. Wang

Ghent University, Ghent, Belgium

V. Adler, K. Beernaert, L. Benucci, A. Cimmino, S. Costantini, S. Crucy, S. Dildick, A. Fagot, G. Garcia, J. Mccartin, A.A. Ocampo Rios, D. Ryckbosch, S. Salva Diblen, M. Sigamani, N. Strobbe, F. Thyssen, M. Tytgat, E. Yazgan, N. Zaganidis

Université Catholique de Louvain, Louvain-la-Neuve, Belgium

S. Basegmez, C. Beluffi³, G. Bruno, R. Castello, A. Caudron, L. Ceard, G.G. Da Silveira, C. Delaere, T. du Pree, D. Favart, L. Forthomme, A. Giammanco⁴, J. Hollar, P. Jez, M. Komm, V. Lemaitre, C. Nuttens, D. Pagano, L. Perrini, A. Pin, K. Piotrkowski, A. Popov⁵, L. Quertenmont, M. Selvaggi, M. Vidal Marono, J.M. Vizan Garcia

Université de Mons, Mons, Belgium

N. Belyi, T. Caebergs, E. Daubie, G.H. Hammad

Centro Brasileiro de Pesquisas Fisicas, Rio de Janeiro, Brazil

W.L. Aldá Júnior, G.A. Alves, L. Brito, M. Correa Martins Junior, M.E. Pol

Universidade do Estado do Rio de Janeiro, Rio de Janeiro, Brazil

W. Carvalho, J. Chinellato⁶, A. Custódio, E.M. Da Costa, D. De Jesus Damiao, C. De Oliveira Martins, S. Fonseca De Souza, H. Malbouisson, D. Matos Figueiredo, L. Mundim, H. Nogima, W.L. Prado Da Silva, J. Santaolalla, A. Santoro, A. Sznajder, E.J. Tonelli Manganote⁶, A. Vilela Pereira

Universidade Estadual Paulista^a, Universidade Federal do ABC^b, São Paulo, Brazil

C.A. Bernardes^b, T.R. Fernandez Perez Tomei^a, E.M. Gregores^b, P.G. Mercadante^b, S.F. Novaes^a, Sandra S. Padula^a

Institute for Nuclear Research and Nuclear Energy, Sofia, Bulgaria

A. Aleksandrov, V. Genchev², P. Iaydjiev, A. Marinov, S. Piperov, M. Rodozov, G. Sultanov, M. Vutova

University of Sofia, Sofia, Bulgaria

A. Dimitrov, I. Glushkov, R. Hadjiiska, V. Kozhuharov, L. Litov, B. Pavlov, P. Petkov

Institute of High Energy Physics, Beijing, China

J.G. Bian, G.M. Chen, H.S. Chen, M. Chen, R. Du, C.H. Jiang, D. Liang, S. Liang, R. Plestina⁷, J. Tao, X. Wang, Z. Wang

State Key Laboratory of Nuclear Physics and Technology, Peking University, Beijing, China

C. Asawatangtrakuldee, Y. Ban, Y. Guo, Q. Li, W. Li, S. Liu, Y. Mao, S.J. Qian, D. Wang, L. Zhang, W. Zou

Universidad de Los Andes, Bogota, Colombia

C. Avila, L.F. Chaparro Sierra, C. Florez, J.P. Gomez, B. Gomez Moreno, J.C. Sanabria

University of Split, Faculty of Electrical Engineering, Mechanical Engineering and Naval Architecture, Split, Croatia

N. Godinovic, D. Lelas, D. Polic, I. Puljak

University of Split, Faculty of Science, Split, Croatia

Z. Antunovic, M. Kovac

Institute Rudjer Boskovic, Zagreb, Croatia

V. Brigljevic, K. Kadija, J. Luetic, D. Mekterovic, L. Sudic

University of Cyprus, Nicosia, Cyprus

A. Attikis, G. Mavromanolakis, J. Mousa, C. Nicolaou, F. Ptochos, P.A. Razis

Charles University, Prague, Czech Republic

M. Bodlak, M. Finger, M. Finger Jr.⁸

Academy of Scientific Research and Technology of the Arab Republic of Egypt, Egyptian Network of High Energy Physics, Cairo, Egypt

Y. Assran⁹, A. Ellithi Kamel¹⁰, M.A. Mahmoud¹¹, A. Radi^{12,13}

National Institute of Chemical Physics and Biophysics, Tallinn, Estonia

M. Kadastik, M. Murumaa, M. Raidal, A. Tiko

Department of Physics, University of Helsinki, Helsinki, Finland

P. Eerola, G. Fedi, M. Voutilainen

Helsinki Institute of Physics, Helsinki, Finland

J. Härkönen, V. Karimäki, R. Kinnunen, M.J. Kortelainen, T. Lampén, K. Lassila-Perini, S. Lehti, T. Lindén, P. Luukka, T. Mäenpää, T. Peltola, E. Tuominen, J. Tuominiemi, E. Tuovinen, L. Wendland

Lappeenranta University of Technology, Lappeenranta, Finland

T. Tuuva

DSM/IRFU, CEA/Saclay, Gif-sur-Yvette, France

M. Besancon, F. Couderc, M. Dejardin, D. Denegri, B. Fabbro, J.L. Faure, C. Favaro, F. Ferri, S. Ganjour, A. Givernaud, P. Gras, G. Hamel de Monchenault, P. Jarry, E. Locci, J. Malcles, J. Rander, A. Rosowsky, M. Titov

Laboratoire Leprince-Ringuet, Ecole Polytechnique, IN2P3-CNRS, Palaiseau, France

S. Baffioni, F. Beaudette, P. Busson, C. Charlot, T. Dahms, M. Dalchenko, L. Dobrzynski, N. Filipovic, A. Florent, R. Granier de Cassagnac, L. Mastrolorenzo, P. Miné, C. Mironov, I.N. Naranjo, M. Nguyen, C. Ochando, P. Paganini, R. Salerno, J.B. Sauvan, Y. Sirois, C. Veelken, Y. Yilmaz, A. Zabi

Institut Pluridisciplinaire Hubert Curien, Université de Strasbourg, Université de Haute Alsace Mulhouse, CNRS/IN2P3, Strasbourg, France

J.-L. Agram¹⁴, J. Andrea, A. Aubin, D. Bloch, J.-M. Brom, E.C. Chabert, C. Collard, E. Conte¹⁴, J.-C. Fontaine¹⁴, D. Gelé, U. Goerlach, C. Goetzmann, A.-C. Le Bihan, P. Van Hove

Centre de Calcul de l'Institut National de Physique Nucleaire et de Physique des Particules, CNRS/IN2P3, Villeurbanne, France

S. Gadrat

Université de Lyon, Université Claude Bernard Lyon 1, CNRS-IN2P3, Institut de Physique Nucléaire de Lyon, Villeurbanne, France

S. Beauceron, N. Beaupere, G. Boudoul², S. Brochet, C.A. Carrillo Montoya, J. Chasserat, R. Chierici, D. Contardo², P. Depasse, H. El Mamouni, J. Fan, J. Fay, S. Gascon, M. Gouzevitch, B. Ille, T. Kurca, M. Lethuillier, L. Mirabito, S. Perries, J.D. Ruiz Alvarez, D. Sabes, L. Sgandurra, V. Sordini, M. Vander Donckt, P. Verdier, S. Viret, H. Xiao

Institute of High Energy Physics and Informatization, Tbilisi State University, Tbilisi, Georgia

I. Bagaturia

RWTH Aachen University, I. Physikalisches Institut, Aachen, Germany

C. Autermann, S. Beranek, M. Bontenackels, M. Edelhoff, L. Feld, O. Hindrichs, K. Klein, A. Ostapchuk, A. Perieanu, F. Raupach, J. Sammet, S. Schael, H. Weber, B. Wittmer, V. Zhukov⁵

RWTH Aachen University, III. Physikalisches Institut A, Aachen, Germany

M. Ata, E. Dietz-Laursonn, D. Duchardt, M. Erdmann, R. Fischer, A. Güth, T. Hebbeker, C. Heidemann, K. Hoepfner, D. Klingebiel, S. Knutzen, P. Kreuzer, M. Merschmeyer, A. Meyer, M. Olschewski, K. Padeken, P. Papacz, H. Reithler, S.A. Schmitz, L. Sonnenschein, D. Teyssier, S. Thüer, M. Weber

RWTH Aachen University, III. Physikalisches Institut B, Aachen, Germany

V. Cherepanov, Y. Erdogan, G. Flügge, H. Geenen, M. Geisler, W. Haj Ahmad, F. Hoehle, B. Kargoll, T. Kress, Y. Kuessel, J. Lingemann², A. Nowack, I.M. Nugent, L. Perchalla, O. Pooth, A. Stahl

Deutsches Elektronen-Synchrotron, Hamburg, Germany

I. Asin, N. Bartosik, J. Behr, W. Behrenhoff, U. Behrens, A.J. Bell, M. Bergholz¹⁵, A. Bethani, K. Borras, A. Burgmeier, A. Cakir, L. Calligaris, A. Campbell, S. Choudhury, F. Costanza, C. Diez Pardos, S. Dooling, T. Dorland, G. Eckerlin, D. Eckstein, T. Eichhorn, G. Flucke, J. Garay Garcia, A. Geiser, P. Gunnellini, J. Hauk, M. Hempel, D. Horton, H. Jung, A. Kalogeropoulos, M. Kasemann, P. Katsas, J. Kieseler, C. Kleinwort, D. Krücker, W. Lange, J. Leonard, K. Lipka, A. Lobanov, W. Lohmann¹⁵, B. Lutz, R. Mankel, I. Marfin, I.-A. Melzer-Pellmann, A.B. Meyer, G. Mittag, J. Mnich, A. Mussgiller, S. Naumann-Emme, A. Nayak, O. Novgorodova, F. Nowak, E. Ntomari, H. Perrey, D. Pitzl, R. Placakyte, A. Raspereza, P.M. Ribeiro Cipriano, E. Ron, M.Ö. Sahin, J. Salfeld-Nebgen, P. Saxena, R. Schmidt¹⁵, T. Schoerner-Sadenius, M. Schröder, C. Seitz, S. Spannagel, A.D.R. Vargas Trevino, R. Walsh, C. Wissing

University of Hamburg, Hamburg, Germany

M. Aldaya Martin, V. Blobel, M. Centis Vignali, A.R. Draeger, J. Erfle, E. Garutti, K. Goebel, M. Görner, J. Haller, M. Hoffmann, R.S. Höing, H. Kirschenmann, R. Klanner, R. Kogler, J. Lange, T. Lapsien, T. Lenz, I. Marchesini, J. Ott, T. Peiffer, N. Pietsch, J. Poehlsen¹⁶, D. Rathjens, C. Sander, H. Schettler, P. Schleper, E. Schlieckau, A. Schmidt, M. Seidel, V. Sola, H. Stadie, G. Steinbrück, D. Troendle, E. Usai, L. Vanelderren

Institut für Experimentelle Kernphysik, Karlsruhe, Germany

C. Barth, C. Baus, J. Berger, C. Böser, E. Butz, T. Chwalek, W. De Boer, A. Descroix, A. Dierlamm, M. Feindt, F. Frensch, M. Giffels, F. Hartmann², T. Hauth², U. Husemann, I. Katkov⁵, A. Kornmayer², E. Kuznetsova, P. Lobelle Pardo, M.U. Mozer, Th. Müller, A. Nürnberg, G. Quast, K. Rabbertz, F. Ratnikov, S. Röcker, H.J. Simonis, F.M. Stober, R. Ulrich, J. Wagner-Kuhr, S. Wayand, T. Weiler, R. Wolf

Institute of Nuclear and Particle Physics (INPP), NCSR Demokritos, Aghia Paraskevi, Greece

G. Anagnostou, G. Daskalakis, T. Gerasis, V.A. Giakoumopoulou, A. Kyriakis, D. Loukas, A. Markou, C. Markou, A. Psallidas, I. Topsis-Giotis

University of Athens, Athens, Greece

A. Agapitos, A. Panagiotou, N. Saoulidou, E. Stiliaris

University of Ioánnina, Ioánnina, Greece

X. Aslanoglou, I. Evangelou, G. Flouris, C. Foudas, P. Kokkas, N. Manthos, I. Papadopoulos, E. Paradas

Wigner Research Centre for Physics, Budapest, Hungary

G. Bencze, C. Hajdu, P. Hidas, D. Horvath¹⁷, F. Sikler, V. Veszpremi, G. Vesztergombi¹⁸, A.J. Zsigmond

Institute of Nuclear Research ATOMKI, Debrecen, Hungary

N. Beni, S. Czellar, J. Karancsi¹⁹, J. Molnar, J. Palinkas, Z. Szillasi

University of Debrecen, Debrecen, Hungary

P. Raics, Z.L. Trocsanyi, B. Ujvari

National Institute of Science Education and Research, Bhubaneswar, India

S.K. Swain

Panjab University, Chandigarh, India

S.B. Beri, V. Bhatnagar, N. Dhingra, R. Gupta, U.Bhawandeep, A.K. Kalsi, M. Kaur, M. Mittal, N. Nishu, J.B. Singh

University of Delhi, Delhi, India

Ashok Kumar, Arun Kumar, S. Ahuja, A. Bhardwaj, B.C. Choudhary, A. Kumar, S. Malhotra, M. Naimuddin, K. Ranjan, V. Sharma

Saha Institute of Nuclear Physics, Kolkata, India

S. Banerjee, S. Bhattacharya, K. Chatterjee, S. Dutta, B. Gomber, Sa. Jain, Sh. Jain, R. Khurana, A. Modak, S. Mukherjee, D. Roy, S. Sarkar, M. Sharan

Bhabha Atomic Research Centre, Mumbai, India

A. Abdulsalam, D. Dutta, S. Kailas, V. Kumar, A.K. Mohanty², L.M. Pant, P. Shukla, A. Topkar

Tata Institute of Fundamental Research, Mumbai, India

T. Aziz, S. Banerjee, S. Bhowmik²⁰, R.M. Chatterjee, R.K. Dewanjee, S. Dugad, S. Ganguly, S. Ghosh, M. Guchait, A. Gurtu²¹, G. Kole, S. Kumar, M. Maity²⁰, G. Majumder, K. Mazumdar, G.B. Mohanty, B. Parida, K. Sudhakar, N. Wickramage²²

Institute for Research in Fundamental Sciences (IPM), Tehran, Iran

H. Bakhshiansohi, H. Behnamian, S.M. Etesami²³, A. Fahim²⁴, R. Goldouzian, A. Jafari, M. Khakzad, M. Mohammadi Najafabadi, M. Naseri, S. Paktinat Mehdiabadi, B. Safarzadeh²⁵, M. Zeinali

University College Dublin, Dublin, Ireland

M. Felcini, M. Grunewald

INFN Sezione di Bari^a, Università di Bari^b, Politecnico di Bari^c, Bari, ItalyM. Abbrescia^{a,b}, L. Barbone^{a,b}, C. Calabria^{a,b}, S.S. Chhibra^{a,b}, A. Colaleo^a, D. Creanza^{a,c}, N. De Filippis^{a,c}, M. De Palma^{a,b}, L. Fiore^a, G. Iaselli^{a,c}, G. Maggi^{a,c}, M. Maggi^a, S. My^{a,c}, S. Nuzzo^{a,b}, A. Pompili^{a,b}, G. Pugliese^{a,c}, R. Radogna^{a,b,2}, G. Selvaggi^{a,b}, L. Silvestris^{a,2}, G. Singh^{a,b}, R. Venditti^{a,b}, P. Verwilligen^a, G. Zito^a**INFN Sezione di Bologna^a, Università di Bologna^b, Bologna, Italy**G. Abbiendi^a, A.C. Benvenuti^a, D. Bonacorsi^{a,b}, S. Braibant-Giacomelli^{a,b}, L. Brigliadori^{a,b}, R. Campanini^{a,b}, P. Capiluppi^{a,b}, A. Castro^{a,b}, F.R. Cavallo^a, G. Codispoti^{a,b}, M. Cuffiani^{a,b}, G.M. Dallavalle^a, F. Fabbri^a, A. Fanfani^{a,b}, D. Fasanella^{a,b}, P. Giacomelli^a, C. Grandi^a, L. Guiducci^{a,b}, S. Marcellini^a, G. Masetti^{a,2}, A. Montanari^a, F.L. Navarria^{a,b}, A. Perrotta^a, F. Primavera^{a,b}, A.M. Rossi^{a,b}, T. Rovelli^{a,b}, G.P. Siroli^{a,b}, N. Tosi^{a,b}, R. Travaglini^{a,b}**INFN Sezione di Catania^a, Università di Catania^b, CSFNMS^c, Catania, Italy**S. Albergo^{a,b}, G. Cappello^a, M. Chiorboli^{a,b}, S. Costa^{a,b}, F. Giordano^{a,2}, R. Potenza^{a,b}, A. Tricomi^{a,b}, C. Tuve^{a,b}**INFN Sezione di Firenze^a, Università di Firenze^b, Firenze, Italy**G. Barbagli^a, V. Ciulli^{a,b}, C. Civinini^a, R. D'Alessandro^{a,b}, E. Focardi^{a,b}, E. Gallo^a, S. Gonzi^{a,b}, V. Gori^{a,b,2}, P. Lenzi^{a,b}, M. Meschini^a, S. Paoletti^a, G. Sguazzoni^a, A. Tropiano^{a,b}**INFN Laboratori Nazionali di Frascati, Frascati, Italy**

L. Benussi, S. Bianco, F. Fabbri, D. Piccolo

INFN Sezione di Genova^a, Università di Genova^b, Genova, ItalyF. Ferro^a, M. Lo Vetere^{a,b}, E. Robutti^a, S. Tosi^{a,b}**INFN Sezione di Milano-Bicocca^a, Università di Milano-Bicocca^b, Milano, Italy**M.E. Dinardo^{a,b}, S. Fiorendi^{a,b,2}, S. Gennai^{a,2}, R. Gerosa^{a,b,2}, A. Ghezzi^{a,b}, P. Govoni^{a,b}, M.T. Lucchini^{a,b,2}, S. Malvezzi^a, R.A. Manzoni^{a,b}, A. Martelli^{a,b}, B. Marzocchi^{a,b}, D. Menasce^a, L. Moroni^a, M. Paganoni^{a,b}, D. Pedrini^a, S. Ragazzi^{a,b}, N. Redaelli^a, T. Tabarelli de Fatis^{a,b}**INFN Sezione di Napoli^a, Università di Napoli 'Federico II'^b, Università della Basilicata (Potenza)^c, Università G. Marconi (Roma)^d, Napoli, Italy**S. Buontempo^a, N. Cavallo^{a,c}, S. Di Guida^{a,d,2}, F. Fabozzi^{a,c}, A.O.M. Iorio^{a,b}, L. Lista^a, S. Meola^{a,d,2}, M. Merola^a, P. Paolucci^{a,2}**INFN Sezione di Padova^a, Università di Padova^b, Università di Trento (Trento)^c, Padova, Italy**P. Azzi^a, N. Bacchetta^a, D. Bisello^{a,b}, A. Branca^{a,b}, R. Carlin^{a,b}, P. Checchia^a, M. Dall'Osso^{a,b}, T. Dorigo^a, M. Galanti^{a,b}, F. Gasparini^{a,b}, U. Gasparini^{a,b},

P. Giubilato^{a,b}, A. Gozzelino^a, K. Kanishchev^{a,c}, S. Lacaprarà^a, M. Margoni^{a,b}, A.T. Meneguzzo^{a,b}, M. Passaseo^a, J. Pazzini^{a,b}, M. Pegoraro^a, N. Pozzobon^{a,b}, P. Ronchese^{a,b}, E. Torassa^a, M. Tosi^{a,b}, P. Zotto^{a,b}, A. Zucchetta^{a,b}, G. Zumerle^{a,b}

INFN Sezione di Pavia^a, Università di Pavia^b, Pavia, Italy

M. Gabusi^{a,b}, S.P. Ratti^{a,b}, C. Riccardi^{a,b}, P. Salvini^a, P. Vitulo^{a,b}

INFN Sezione di Perugia^a, Università di Perugia^b, Perugia, Italy

M. Biasini^{a,b}, G.M. Bilei^a, D. Ciangottini^{a,b}, L. Fanò^{a,b}, P. Lariccia^{a,b}, G. Mantovani^{a,b}, M. Menichelli^a, F. Romeo^{a,b}, A. Saha^a, A. Santocchia^{a,b}, A. Spiezia^{a,b,2}

INFN Sezione di Pisa^a, Università di Pisa^b, Scuola Normale Superiore di Pisa^c, Pisa, Italy

K. Androsov^{a,26}, P. Azzurri^a, G. Bagliesi^a, J. Bernardini^a, T. Boccali^a, G. Broccolo^{a,c}, R. Castaldi^a, M.A. Ciocci^{a,26}, R. Dell'Orso^a, S. Donato^{a,c}, F. Fiori^{a,c}, L. Foà^{a,c}, A. Giassi^a, M.T. Grippo^{a,26}, F. Ligabue^{a,c}, T. Lomtadze^a, L. Martini^{a,b}, A. Messineo^{a,b}, C.S. Moon^{a,27}, F. Palla^{a,2}, A. Rizzi^{a,b}, A. Savoy-Navarro^{a,28}, A.T. Serban^a, P. Spagnolo^a, P. Squillacioti^{a,26}, R. Tenchini^a, G. Tonelli^{a,b}, A. Venturi^a, P.G. Verdini^a, C. Vernieri^{a,c,2}

INFN Sezione di Roma^a, Università di Roma^b, Roma, Italy

L. Barone^{a,b}, F. Cavallari^a, D. Del Re^{a,b}, M. Diemoz^a, M. Grassi^{a,b}, C. Jorda^a, E. Longo^{a,b}, F. Margaroli^{a,b}, P. Meridiani^a, F. Micheli^{a,b,2}, S. Nourbakhsh^{a,b}, G. Organtini^{a,b}, R. Paramatti^a, S. Rahatlou^{a,b}, C. Rovelli^a, F. Santanastasio^{a,b}, L. Soffi^{a,b,2}, P. Traczyk^{a,b}

INFN Sezione di Torino^a, Università di Torino^b, Università del Piemonte Orientale (Novara)^c, Torino, Italy

N. Amapane^{a,b}, R. Arcidiacono^{a,c}, S. Argiro^{a,b,2}, M. Arneodo^{a,c}, R. Bellan^{a,b}, C. Biino^a, N. Cartiglia^a, S. Casasso^{a,b,2}, M. Costa^{a,b}, A. Degano^{a,b}, N. Demaria^a, L. Finco^{a,b}, C. Mariotti^a, S. Maselli^a, E. Migliore^{a,b}, V. Monaco^{a,b}, M. Musich^a, M.M. Obertino^{a,c,2}, G. Ortona^{a,b}, L. Pacher^{a,b}, N. Pastrone^a, M. Pelliccioni^a, G.L. Pinna Angioni^{a,b}, A. Potenza^{a,b}, A. Romero^{a,b}, M. Ruspa^{a,c}, R. Sacchi^{a,b}, A. Solano^{a,b}, A. Staiano^a, U. Tamponi^a

INFN Sezione di Trieste^a, Università di Trieste^b, Trieste, Italy

S. Belforte^a, V. Candelise^{a,b}, M. Casarsa^a, F. Cossutti^a, G. Della Ricca^{a,b}, B. Gobbo^a, C. La Licata^{a,b}, M. Marone^{a,b}, D. Montanino^{a,b}, A. Schizzi^{a,b,2}, T. Umer^{a,b}, A. Zanetti^a

Kangwon National University, Chunchon, Korea

S. Chang, A. Kropivnitskaya, S.K. Nam

Kyungpook National University, Daegu, Korea

D.H. Kim, G.N. Kim, M.S. Kim, D.J. Kong, S. Lee, Y.D. Oh, H. Park, A. Sakharov, D.C. Son

Chonbuk National University, Jeonju, Korea

T.J. Kim

Chonnam National University, Institute for Universe and Elementary Particles, Kwangju, Korea

J.Y. Kim, S. Song

Korea University, Seoul, Korea

S. Choi, D. Gyun, B. Hong, M. Jo, H. Kim, Y. Kim, B. Lee, K.S. Lee, S.K. Park, Y. Roh

University of Seoul, Seoul, Korea

M. Choi, J.H. Kim, I.C. Park, S. Park, G. Ryu, M.S. Ryu

Sungkyunkwan University, Suwon, Korea

Y. Choi, Y.K. Choi, J. Goh, D. Kim, E. Kwon, J. Lee, H. Seo, I. Yu

Vilnius University, Vilnius, Lithuania

A. Juodagalvis

National Centre for Particle Physics, Universiti Malaya, Kuala Lumpur, Malaysia

J.R. Komaragiri, M.A.B. Md Ali

Centro de Investigacion y de Estudios Avanzados del IPN, Mexico City, Mexico

H. Castilla-Valdez, E. De La Cruz-Burelo, I. Heredia-de La Cruz²⁹, R. Lopez-Fernandez, A. Sanchez-Hernandez

Universidad Iberoamericana, Mexico City, Mexico

S. Carrillo Moreno, F. Vazquez Valencia

Benemerita Universidad Autonoma de Puebla, Puebla, Mexico

I. Pedraza, H.A. Salazar Ibarguen

Universidad Autónoma de San Luis Potosí, San Luis Potosí, Mexico

E. Casimiro Linares, A. Morelos Pineda

University of Auckland, Auckland, New Zealand

D. Krofcheck

University of Canterbury, Christchurch, New Zealand

P.H. Butler, S. Reucroft

National Centre for Physics, Quaid-I-Azam University, Islamabad, Pakistan

A. Ahmad, M. Ahmad, Q. Hassan, H.R. Hoorani, S. Khalid, W.A. Khan, T. Khurshid, M.A. Shah, M. Shoaib

National Centre for Nuclear Research, Swierk, Poland

H. Bialkowska, M. Bluj, B. Boimska, T. Frueboes, M. Górski, M. Kazana, K. Nawrocki, K. Romanowska-Rybinska, M. Szleper, P. Zalewski

Institute of Experimental Physics, Faculty of Physics, University of Warsaw, Warsaw, Poland

G. Brona, K. Bunkowski, M. Cwiok, W. Dominik, K. Doroba, A. Kalinowski, M. Konecki, J. Krolikowski, M. Misiura, M. Olszewski, W. Wolszczak

Laboratório de Instrumentação e Física Experimental de Partículas, Lisboa, Portugal

P. Bargassa, C. Beirão Da Cruz E Silva, P. Faccioli, P.G. Ferreira Parracho, M. Gallinaro, F. Nguyen, J. Rodrigues Antunes, J. Seixas, J. Varela, P. Vischia

Joint Institute for Nuclear Research, Dubna, Russia

S. Afanasiev, I. Golutvin, V. Karjavin, V. Konoplyanikov, V. Korenkov, G. Kozlov, A. Lanev, A. Malakhov, V. Matveev³⁰, V.V. Mitsyn, P. Moisenz, V. Palichik, V. Perelygin, S. Shmatov, N. Skatchkov, V. Smirnov, E. Tikhonenko, A. Zarubin

Petersburg Nuclear Physics Institute, Gatchina (St. Petersburg), Russia

V. Golovtsov, Y. Ivanov, V. Kim³¹, P. Levchenko, V. Murzin, V. Oreshkin, I. Smirnov, V. Sulimov, L. Uvarov, S. Vavilov, A. Vorobyev, An. Vorobyev

Institute for Nuclear Research, Moscow, Russia

Yu. Andreev, A. Dermenev, S. Gninenko, N. Golubev, M. Kirsanov, N. Krasnikov, A. Pashenkov, D. Tlisov, A. Toropin

Institute for Theoretical and Experimental Physics, Moscow, Russia

V. Epshteyn, V. Gavrilov, N. Lychkovskaya, V. Popov, G. Safronov, S. Semenov, A. Spiridonov, V. Stolin, E. Vlasov, A. Zhokin

P.N. Lebedev Physical Institute, Moscow, Russia

V. Andreev, M. Azarkin, I. Dremin, M. Kirakosyan, A. Leonidov, G. Mesyats, S.V. Rusakov, A. Vinogradov

Skobeltsyn Institute of Nuclear Physics, Lomonosov Moscow State University, Moscow, Russia

A. Belyaev, E. Boos, A. Ershov, A. Gribushin, A. Kaminskiy³², O. Kodolova, V. Korotkikh, I. Lokhtin, S. Obraztsov, S. Petrushanko, V. Savrin, A. Snigirev, I. Vardanyan

State Research Center of Russian Federation, Institute for High Energy Physics, Protvino, Russia

I. Azhgirey, I. Bayshev, S. Bitioukov, V. Kachanov, A. Kalinin, D. Konstantinov, V. Krychkine, V. Petrov, R. Ryutin, A. Sobol, L. Tourtchanovitch, S. Troshin, N. Tyurin, A. Uzunian, A. Volkov

University of Belgrade, Faculty of Physics and Vinca Institute of Nuclear Sciences, Belgrade, Serbia

P. Adzic³³, M. Ekmedzic, J. Milosevic, V. Rekovic

Centro de Investigaciones Energéticas Medioambientales y Tecnológicas (CIEMAT), Madrid, Spain

J. Alcaraz Maestre, C. Battilana, E. Calvo, M. Cerrada, M. Chamizo Llatas, N. Colino, B. De La Cruz, A. Delgado Peris, D. Domínguez Vázquez, A. Escalante Del Valle, C. Fernandez Bedoya, J.P. Fernández Ramos, J. Flix, M.C. Fouz, P. Garcia-Abia, O. Gonzalez Lopez, S. Goy Lopez, J.M. Hernandez, M.I. Josa, G. Merino, E. Navarro De Martino,

A. Pérez-Calero Yzquierdo, J. Puerta Pelayo, A. Quintario Olmeda, I. Redondo, L. Romero, M.S. Soares

Universidad Autónoma de Madrid, Madrid, Spain

C. Albajar, J.F. de Trocóniz, M. Missiroli, D. Moran

Universidad de Oviedo, Oviedo, Spain

H. Brun, J. Cuevas, J. Fernandez Menendez, S. Folgueras, I. Gonzalez Caballero, L. Lloret Iglesias

Instituto de Física de Cantabria (IFCA), CSIC-Universidad de Cantabria, Santander, Spain

J.A. Brochero Cifuentes, I.J. Cabrillo, A. Calderon, J. Duarte Campderros, M. Fernandez, G. Gomez, A. Graziano, A. Lopez Virto, J. Marco, R. Marco, C. Martinez Rivero, F. Matorras, F.J. Munoz Sanchez, J. Piedra Gomez, T. Rodrigo, A.Y. Rodríguez-Marrero, A. Ruiz-Jimeno, L. Scodellaro, I. Vila, R. Vilar Cortabitarte

CERN, European Organization for Nuclear Research, Geneva, Switzerland

D. Abbaneo, E. Auffray, G. Auzinger, M. Bachtis, P. Baillon, A.H. Ball, D. Barney, A. Benaglia, J. Bendavid, L. Benhabib, J.F. Benitez, C. Bernet⁷, G. Bianchi, P. Bloch, A. Bocci, A. Bonato, O. Bondu, C. Botta, H. Breuker, T. Camporesi, G. Cerminara, S. Colafranceschi³⁴, M. D'Alfonso, D. d'Enterria, A. Dabrowski, A. David, F. De Guio, A. De Roeck, S. De Visscher, M. Dobson, M. Dordevic, N. Dupont-Sagorin, A. Elliott-Peisert, J. Eugster, G. Franzoni, W. Funk, D. Gigi, K. Gill, D. Giordano, M. Girone, F. Glege, R. Guida, S. Gundacker, M. Guthoff, J. Hammer, M. Hansen, P. Harris, J. Hege-
man, V. Innocente, P. Janot, K. Kousouris, K. Krajczar, P. Lecoq, C. Lourenço, N. Magini, L. Malgeri, M. Mannelli, J. Marrouche, L. Masetti, F. Meijers, S. Mersi, E. Meschi, F. Moortgat, S. Morovic, M. Mulders, P. Musella, L. Orsini, L. Pape, E. Perez, L. Perrozzi, A. Petrilli, G. Petrucciani, A. Pfeiffer, M. Pierini, M. Pimiä, D. Piparo, M. Plagge, A. Racz, G. Rolandi³⁵, M. Rovere, H. Sakulin, C. Schäfer, C. Schwick, A. Sharma, P. Siegrist, P. Silva, M. Simon, P. Sphicas³⁶, D. Spiga, J. Steggemann, B. Stieger, M. Stoye, D. Treille, A. Tsirou, G.I. Veres¹⁸, J.R. Vlimant, N. Wardle, H.K. Wöhri, H. Wollny, W.D. Zeuner

Paul Scherrer Institut, Villigen, Switzerland

W. Bertl, K. Deiters, W. Erdmann, R. Horisberger, Q. Ingram, H.C. Kaestli, S. König, D. Kotlinski, U. Langenegger, D. Renker, T. Rohe

Institute for Particle Physics, ETH Zurich, Zurich, Switzerland

F. Bachmair, L. Bäni, L. Bianchini, P. Bortignon, M.A. Buchmann, B. Casal, N. Chanon, A. Deisher, G. Dissertori, M. Dittmar, M. Donegà, M. Dünser, P. Eller, C. Grab, D. Hits, W. Lustermann, B. Mangano, A.C. Marini, P. Martinez Ruiz del Arbol, D. Meister, N. Mohr, C. Nägeli³⁷, F. Nessi-Tedaldi, F. Pandolfi, F. Pauss, M. Peruzzi, M. Quittnat, L. Rebane, M. Rossini, A. Starodumov³⁸, M. Takahashi, K. Theofilatos, R. Wallny, H.A. Weber

Universität Zürich, Zurich, Switzerland

C. AMSLER³⁹, M.F. Canelli, V. Chiochia, A. De Cosa, A. Hinzmann, T. Hreus, B. Kilminster, B. Millan Mejias, J. Ngadiuba, P. Robmann, F.J. Ronga, S. Taroni, M. Verzetti, Y. Yang

National Central University, Chung-Li, Taiwan

M. Cardaci, K.H. Chen, C. Ferro, C.M. Kuo, W. Lin, Y.J. Lu, R. Volpe, S.S. Yu

National Taiwan University (NTU), Taipei, Taiwan

P. Chang, Y.H. Chang, Y.W. Chang, Y. Chao, K.F. Chen, P.H. Chen, C. Dietz, U. Grundler, W.-S. Hou, K.Y. Kao, Y.J. Lei, Y.F. Liu, R.-S. Lu, D. Majumder, E. Petrakou, Y.M. Tzeng, R. Wilken

Chulalongkorn University, Faculty of Science, Department of Physics, Bangkok, Thailand

B. Asavapibhop, N. Srimanobhas, N. Suwonjandee

Cukurova University, Adana, Turkey

A. Adiguzel, M.N. Bakirci⁴⁰, S. Cerci⁴¹, C. Dozen, I. Dumanoglu, E. Eskut, S. Girgis, G. Gokbulut, E. Gurpinar, I. Hos, E.E. Kangal, A. Kayis Topaksu, G. Onengut⁴², K. Ozdemir, S. Ozturk⁴⁰, A. Polatoz, K. Sogut⁴³, D. Sunar Cerci⁴¹, B. Tali⁴¹, H. Topakli⁴⁰, M. Vergili

Middle East Technical University, Physics Department, Ankara, Turkey

I.V. Akin, B. Bilin, S. Bilmis, H. Gamsizkan, G. Karapinar⁴⁴, K. Ocalan, S. Sekmen, U.E. Surat, M. Yalvac, M. Zeyrek

Bogazici University, Istanbul, Turkey

E. Gülmez, B. Isildak⁴⁵, M. Kaya⁴⁶, O. Kaya⁴⁶

Istanbul Technical University, Istanbul, Turkey

H. Bahtiyar⁴⁷, E. Barlas, K. Cankocak, F.I. Vardarli, M. Yücel

National Scientific Center, Kharkov Institute of Physics and Technology, Kharkov, Ukraine

L. Levchuk, P. Sorokin

University of Bristol, Bristol, United Kingdom

J.J. Brooke, E. Clement, D. Cussans, H. Flacher, R. Frazier, J. Goldstein, M. Grimes, G.P. Heath, H.F. Heath, J. Jacob, L. Kreczko, C. Lucas, Z. Meng, D.M. Newbold⁴⁸, S. Paramesvaran, A. Poll, S. Senkin, V.J. Smith, T. Williams

Rutherford Appleton Laboratory, Didcot, United Kingdom

A. Belyaev⁴⁹, C. Brew, R.M. Brown, D.J.A. Cockerill, J.A. Coughlan, K. Harder, S. Harper, E. Olaiya, D. Petyt, C.H. Shepherd-Themistocleous, A. Thea, I.R. Tomalin, W.J. Womersley, S.D. Worm

Imperial College, London, United Kingdom

M. Baber, R. Bainbridge, O. Buchmuller, D. Burton, D. Colling, N. Cripps, M. Cutajar, P. Dauncey, G. Davies, M. Della Negra, P. Dunne, W. Ferguson, J. Fulcher, D. Futyan,

A. Gilbert, G. Hall, G. Iles, M. Jarvis, G. Karapostoli, M. Kenzie, R. Lane, R. Lucas⁴⁸, L. Lyons, A.-M. Magnan, S. Malik, B. Mathias, J. Nash, A. Nikitenko³⁸, J. Pela, M. Pesaresi, K. Petridis, D.M. Raymond, S. Rogerson, A. Rose, C. Seez, P. Sharp[†], A. Tapper, M. Vazquez Acosta, T. Virdee

Brunel University, Uxbridge, United Kingdom

J.E. Cole, P.R. Hobson, A. Khan, P. Kyberd, D. Leggat, D. Leslie, W. Martin, I.D. Reid, P. Symonds, L. Teodorescu, M. Turner

Baylor University, Waco, USA

J. Dittmann, K. Hatakeyama, A. Kasmi, H. Liu, T. Scarborough

The University of Alabama, Tuscaloosa, USA

O. Charaf, S.I. Cooper, C. Henderson, P. Rumerio

Boston University, Boston, USA

A. Avetisyan, T. Bose, C. Fantasia, A. Heister, P. Lawson, C. Richardson, J. Rohlf, D. Sperka, J. St. John, L. Sulak

Brown University, Providence, USA

J. Alimena, E. Berry, S. Bhattacharya, G. Christopher, D. Cutts, Z. Demiragli, A. Ferapontov, A. Garabedian, U. Heintz, G. Kukartsev, E. Laird, G. Landsberg, M. Luk, M. Narain, M. Segala, T. Sinthuprasith, T. Speer, J. Swanson

University of California, Davis, Davis, USA

R. Breedon, G. Breto, M. Calderon De La Barca Sanchez, S. Chauhan, M. Chertok, J. Conway, R. Conway, P.T. Cox, R. Erbacher, M. Gardner, W. Ko, R. Lander, T. Miceli, M. Mulhearn, D. Pellett, J. Pilot, F. Ricci-Tam, M. Searle, S. Shalhout, J. Smith, M. Squires, D. Stolp, M. Tripathi, S. Wilbur, R. Yohay

University of California, Los Angeles, USA

R. Cousins, P. Everaerts, C. Farrell, J. Hauser, M. Ignatenko, G. Rakness, E. Takasugi, V. Valuev, M. Weber

University of California, Riverside, Riverside, USA

J. Babb, K. Burt, R. Clare, J. Ellison, J.W. Gary, G. Hanson, J. Heilman, M. Ivova Rikova, P. Jandir, E. Kennedy, F. Lacroix, H. Liu, O.R. Long, A. Luthra, M. Malberti, H. Nguyen, M. Olmedo Negrete, A. Shrinivas, S. Sumowidagdo, S. Wimpenny

University of California, San Diego, La Jolla, USA

W. Andrews, J.G. Branson, G.B. Cerati, S. Cittolin, R.T. D’Agnolo, D. Evans, A. Holzner, R. Kelley, D. Klein, M. Lebourgeois, J. Letts, I. Macneill, D. Olivito, S. Padhi, C. Palmer, M. Pieri, M. Sani, V. Sharma, S. Simon, E. Sudano, M. Tadel, Y. Tu, A. Vartak, C. Welke, F. Würthwein, A. Yagil, J. Yoo

University of California, Santa Barbara, Santa Barbara, USA

D. Barge, J. Bradmiller-Feld, C. Campagnari, T. Danielson, A. Dishaw, K. Flowers, M. Franco Sevilla, P. Geffert, C. George, F. Golf, L. Gouskos, J. Incandela, C. Justus, N. Mccoll, J. Richman, D. Stuart, W. To, C. West

California Institute of Technology, Pasadena, USA

A. Apresyan, A. Bornheim, J. Bunn, Y. Chen, E. Di Marco, J. Duarte, A. Mott, H.B. Newman, C. Pena, C. Rogan, M. Spiropulu, V. Timciuc, R. Wilkinson, S. Xie, R.Y. Zhu

Carnegie Mellon University, Pittsburgh, USA

V. Azzolini, A. Calamba, T. Ferguson, Y. Iiyama, M. Paulini, J. Russ, H. Vogel, I. Vorobiev

University of Colorado at Boulder, Boulder, USA

J.P. Cumalat, W.T. Ford, A. Gaz, E. Luigi Lopez, U. Nauenberg, J.G. Smith, K. Stenson, K.A. Ulmer, S.R. Wagner

Cornell University, Ithaca, USA

J. Alexander, A. Chatterjee, J. Chu, S. Dittmer, N. Eggert, N. Mirman, G. Nicolas Kaufman, J.R. Patterson, A. Ryd, E. Salvati, L. Skinnari, W. Sun, W.D. Teo, J. Thom, J. Thompson, J. Tucker, Y. Weng, L. Winstrom, P. Wittich

Fairfield University, Fairfield, USA

D. Winn

Fermi National Accelerator Laboratory, Batavia, USA

S. Abdullin, M. Albrow, J. Anderson, G. Apollinari, L.A.T. Bauerdick, A. Beretvas, J. Berryhill, P.C. Bhat, K. Burkett, J.N. Butler, H.W.K. Cheung, F. Chlebana, S. Cihangir, V.D. Elvira, I. Fisk, J. Freeman, Y. Gao, E. Gottschalk, L. Gray, D. Green, S. Grünendahl, O. Gutsche, J. Hanlon, D. Hare, R.M. Harris, J. Hirschauer, B. Hooberman, S. Jindariani, M. Johnson, U. Joshi, K. Kaadze, B. Klima, B. Kreis, S. Kwan, J. Linacre, D. Lincoln, R. Lipton, T. Liu, J. Lykken, K. Maeshima, J.M. Marraffino, V.I. Martinez Outschoorn, S. Maruyama, D. Mason, P. McBride, K. Mishra, S. Mrenna, Y. Musienko³⁰, S. Nahn, C. Newman-Holmes, V. O'Dell, O. Prokofyev, E. Sexton-Kennedy, S. Sharma, A. Soha, W.J. Spalding, L. Spiegel, L. Taylor, S. Tkaczyk, N.V. Tran, L. Uplegger, E.W. Vaandering, R. Vidal, A. Whitbeck, J. Whitmore, F. Yang

University of Florida, Gainesville, USA

D. Acosta, P. Avery, D. Bourilkov, M. Carver, T. Cheng, D. Curry, S. Das, M. De Gruttola, G.P. Di Giovanni, R.D. Field, M. Fisher, I.K. Furic, J. Hugon, J. Konigsberg, A. Korytov, T. Kypreos, J.F. Low, K. Matchev, P. Milenovic⁵⁰, G. Mitselmakher, L. Muniz, A. Rinkevicius, L. Shchutska, N. Skhirtladze, M. Snowball, J. Yelton, M. Zakaria

Florida International University, Miami, USA

S. Hewamanage, S. Linn, P. Markowitz, G. Martinez, J.L. Rodriguez

Florida State University, Tallahassee, USA

T. Adams, A. Askew, J. Bochenek, B. Diamond, J. Haas, S. Hagopian, V. Hagopian, K.F. Johnson, H. Prosper, V. Veeraraghavan, M. Weinberg

Florida Institute of Technology, Melbourne, USA

M.M. Baarmand, M. Hohlmann, H. Kalakhety, F. Yumiceva

University of Illinois at Chicago (UIC), Chicago, USA

M.R. Adams, L. Apanasevich, V.E. Bazterra, D. Berry, R.R. Betts, I. Bucinskaite, R. Cavanaugh, O. Evdokimov, L. Gauthier, C.E. Gerber, D.J. Hofman, S. Khalatyan, P. Kurt, D.H. Moon, C. O'Brien, C. Silkworth, P. Turner, N. Varelas

The University of Iowa, Iowa City, USA

E.A. Albayrak⁴⁷, B. Bilki⁵¹, W. Clarida, K. Dilsiz, F. Duru, M. Haytmyradov, J.-P. Merlo, H. Mermerkaya⁵², A. Mestvirishvili, A. Moeller, J. Nachtman, H. Ogul, Y. Onel, F. Ozok⁴⁷, A. Penzo, R. Rahmat, S. Sen, P. Tan, E. Tiras, J. Wetzel, T. Yetkin⁵³, K. Yi

Johns Hopkins University, Baltimore, USA

B.A. Barnett, B. Blumenfeld, S. Bolognesi, D. Fehling, A.V. Gritsan, P. Maksimovic, C. Martin, M. Swartz

The University of Kansas, Lawrence, USA

P. Baringer, A. Bean, G. Benelli, C. Bruner, J. Gray, R.P. Kenny III, M. Malek, M. Murray, D. Noonan, S. Sanders, J. Sekaric, R. Stringer, Q. Wang, J.S. Wood

Kansas State University, Manhattan, USA

A.F. Barfuss, I. Chakaberia, A. Ivanov, S. Khalil, M. Makouski, Y. Maravin, L.K. Saini, S. Shrestha, I. Svintradze

Lawrence Livermore National Laboratory, Livermore, USA

J. Gronberg, D. Lange, F. Rebassoo, D. Wright

University of Maryland, College Park, USA

A. Baden, A. Belloni, B. Calvert, S.C. Eno, J.A. Gomez, N.J. Hadley, R.G. Kellogg, T. Kolberg, Y. Lu, M. Marionneau, A.C. Mignerey, K. Pedro, A. Skuja, M.B. Tonjes, S.C. Tonwar

Massachusetts Institute of Technology, Cambridge, USA

A. Apyan, R. Barbieri, G. Bauer, W. Busza, I.A. Cali, M. Chan, L. Di Matteo, V. Dutta, G. Gomez Ceballos, M. Goncharov, D. Gulhan, M. Klute, Y.S. Lai, Y.-J. Lee, A. Levin, P.D. Luckey, T. Ma, C. Paus, D. Ralph, C. Roland, G. Roland, G.S.F. Stephans, F. Stöckli, K. Sumorok, D. Velicanu, J. Veverka, B. Wyslouch, M. Yang, M. Zanetti, V. Zhukova

University of Minnesota, Minneapolis, USA

B. Dahmes, A. Gude, S.C. Kao, K. Klapoetke, Y. Kubota, J. Mans, N. Pastika, R. Rusack, A. Singovsky, N. Tambe, J. Turkewitz

University of Mississippi, Oxford, USA

J.G. Acosta, S. Oliveros

University of Nebraska-Lincoln, Lincoln, USA

E. Avdeeva, K. Bloom, S. Bose, D.R. Claes, A. Dominguez, R. Gonzalez Suarez, J. Keller, D. Knowlton, I. Kravchenko, J. Lazo-Flores, S. Malik, F. Meier, G.R. Snow

State University of New York at Buffalo, Buffalo, USA

J. Dolen, A. Godshalk, I. Iashvili, A. Kharchilava, A. Kumar, S. Rappoccio

Northeastern University, Boston, USA

G. Alverson, E. Barberis, D. Baumgartel, M. Chasco, J. Haley, A. Massironi, D.M. Morse, D. Nash, T. Orimoto, D. Trocino, R.-J. Wang, D. Wood, J. Zhang

Northwestern University, Evanston, USA

K.A. Hahn, A. Kubik, N. Mucia, N. Odell, B. Pollack, A. Pozdnyakov, M. Schmitt, S. Stoynev, K. Sung, M. Velasco, S. Won

University of Notre Dame, Notre Dame, USA

A. Brinkerhoff, K.M. Chan, A. Drozdetskiy, M. Hildreth, C. Jessop, D.J. Karmgard, N. Kellams, K. Lannon, W. Luo, S. Lynch, N. Marinelli, T. Pearson, M. Planer, R. Ruchti, N. Valls, M. Wayne, M. Wolf, A. Woodard

The Ohio State University, Columbus, USA

L. Antonelli, J. Brinson, B. Bylsma, L.S. Durkin, S. Flowers, C. Hill, R. Hughes, K. Kotov, T.Y. Ling, D. Puigh, M. Rodenburg, G. Smith, C. Vuosalo, B.L. Winer, H. Wolfe, H.W. Wulsin

Princeton University, Princeton, USA

O. Driga, P. Elmer, P. Hebda, A. Hunt, S.A. Koay, P. Lujan, D. Marlow, T. Medvedeva, M. Mooney, J. Olsen, P. Piroué, X. Quan, H. Saka, D. Stickland², C. Tully, J.S. Werner, S.C. Zenz, A. Zuranski

University of Puerto Rico, Mayaguez, USA

E. Brownson, H. Mendez, J.E. Ramirez Vargas

Purdue University, West Lafayette, USA

E. Alagoz, V.E. Barnes, D. Benedetti, G. Bolla, D. Bortoletto, M. De Mattia, Z. Hu, M.K. Jha, M. Jones, K. Jung, M. Kress, N. Leonardo, D. Lopes Pegna, V. Maroussov, P. Merkel, D.H. Miller, N. Neumeister, B.C. Radburn-Smith, X. Shi, I. Shipsey, D. Silvers, A. Svyatkovskiy, F. Wang, W. Xie, L. Xu, H.D. Yoo, J. Zablocki, Y. Zheng

Purdue University Calumet, Hammond, USA

N. Parashar, J. Stupak

Rice University, Houston, USA

A. Adair, B. Akgun, K.M. Ecklund, F.J.M. Geurts, W. Li, B. Michlin, B.P. Padley, R. Redjimi, J. Roberts, J. Zabel

University of Rochester, Rochester, USA

B. Betchart, A. Bodek, R. Covarelli, P. de Barbaro, R. Demina, Y. Eshaq, T. Ferbel, A. Garcia-Bellido, P. Goldenzweig, J. Han, A. Harel, A. Khukhunaishvili, G. Petrillo, D. Vishnevskiy

The Rockefeller University, New York, USA

R. Ciesielski, L. Demortier, K. Goulianos, G. Lungu, C. Mesropian

Rutgers, The State University of New Jersey, Piscataway, USA

S. Arora, A. Barker, J.P. Chou, C. Contreras-Campana, E. Contreras-Campana, D. Duggan, D. Ferencek, Y. Gershtein, R. Gray, E. Halkiadakis, D. Hidas, A. Lath, S. Panwalkar, M. Park, R. Patel, S. Salur, S. Schnetzer, S. Somalwar, R. Stone, S. Thomas, P. Thomassen, M. Walker

University of Tennessee, Knoxville, USA

K. Rose, S. Spanier, A. York

Texas A&M University, College Station, USA

O. Bouhali⁵⁴, R. Eusebi, W. Flanagan, J. Gilmore, T. Kamon⁵⁵, V. Khotilovich, V. Krutelyov, R. Montalvo, I. Osipenkov, Y. Pakhotin, A. Perloff, J. Roe, A. Rose, A. Safonov, T. Sakuma, I. Suarez, A. Tatarinov

Texas Tech University, Lubbock, USA

N. Akchurin, C. Cowden, J. Damgov, C. Dragoiu, P.R. Duderø, J. Faulkner, K. Kovitang-goon, S. Kunori, S.W. Lee, T. Libeiro, I. Volobouev

Vanderbilt University, Nashville, USA

E. Appelt, A.G. Delannoy, S. Greene, A. Gurrola, W. Johns, C. Maguire, Y. Mao, A. Melo, M. Sharma, P. Sheldon, B. Snook, S. Tuo, J. Velkovska

University of Virginia, Charlottesville, USA

M.W. Arenton, S. Boutle, B. Cox, B. Francis, J. Goodell, R. Hirosky, A. Ledovskoy, H. Li, C. Lin, C. Neu, J. Wood

Wayne State University, Detroit, USA

R. Harr, P.E. Karchin, C. Kottachchi Kankanamge Don, P. Lamichhane, J. Sturdy

University of Wisconsin, Madison, USA

D.A. Belknap, D. Carlsmith, M. Cepeda, S. Dasu, S. Duric, E. Friis, R. Hall-Wilton, M. Herndon, A. Hervé, P. Klabbers, A. Lanaro, C. Lazaridis, A. Levine, R. Loveless, A. Mohapatra, I. Ojalvo, T. Perry, G.A. Pierro, G. Polese, I. Ross, T. Sarangi, A. Savin, W.H. Smith, N. Woods

†: Deceased

1: Also at Vienna University of Technology, Vienna, Austria

2: Also at CERN, European Organization for Nuclear Research, Geneva, Switzerland

3: Also at Institut Pluridisciplinaire Hubert Curien, Université de Strasbourg, Université de Haute Alsace Mulhouse, CNRS/IN2P3, Strasbourg, France

4: Also at National Institute of Chemical Physics and Biophysics, Tallinn, Estonia

5: Also at Skobeltsyn Institute of Nuclear Physics, Lomonosov Moscow State University, Moscow, Russia

6: Also at Universidade Estadual de Campinas, Campinas, Brazil

7: Also at Laboratoire Leprince-Ringuet, Ecole Polytechnique, IN2P3-CNRS, Palaiseau, France

8: Also at Joint Institute for Nuclear Research, Dubna, Russia

9: Also at Suez University, Suez, Egypt

10: Also at Cairo University, Cairo, Egypt

11: Also at Fayoum University, El-Fayoum, Egypt

- 12: Also at British University in Egypt, Cairo, Egypt
- 13: Now at Sultan Qaboos University, Muscat, Oman
- 14: Also at Université de Haute Alsace, Mulhouse, France
- 15: Also at Brandenburg University of Technology, Cottbus, Germany
- 16: Also at The University of Kansas, Lawrence, USA
- 17: Also at Institute of Nuclear Research ATOMKI, Debrecen, Hungary
- 18: Also at Eötvös Loránd University, Budapest, Hungary
- 19: Also at University of Debrecen, Debrecen, Hungary
- 20: Also at University of Visva-Bharati, Santiniketan, India
- 21: Now at King Abdulaziz University, Jeddah, Saudi Arabia
- 22: Also at University of Ruhuna, Matara, Sri Lanka
- 23: Also at Isfahan University of Technology, Isfahan, Iran
- 24: Also at Sharif University of Technology, Tehran, Iran
- 25: Also at Plasma Physics Research Center, Science and Research Branch, Islamic Azad University, Tehran, Iran
- 26: Also at Università degli Studi di Siena, Siena, Italy
- 27: Also at Centre National de la Recherche Scientifique (CNRS) - IN2P3, Paris, France
- 28: Also at Purdue University, West Lafayette, USA
- 29: Also at Universidad Michoacana de San Nicolas de Hidalgo, Morelia, Mexico
- 30: Also at Institute for Nuclear Research, Moscow, Russia
- 31: Also at St. Petersburg State Polytechnical University, St. Petersburg, Russia
- 32: Also at INFN Sezione di Padova; Università di Padova; Università di Trento (Trento), Padova, Italy
- 33: Also at Faculty of Physics, University of Belgrade, Belgrade, Serbia
- 34: Also at Facoltà Ingegneria, Università di Roma, Roma, Italy
- 35: Also at Scuola Normale e Sezione dell'INFN, Pisa, Italy
- 36: Also at University of Athens, Athens, Greece
- 37: Also at Paul Scherrer Institut, Villigen, Switzerland
- 38: Also at Institute for Theoretical and Experimental Physics, Moscow, Russia
- 39: Also at Albert Einstein Center for Fundamental Physics, Bern, Switzerland
- 40: Also at Gaziosmanpasa University, Tokat, Turkey
- 41: Also at Adiyaman University, Adiyaman, Turkey
- 42: Also at Cag University, Mersin, Turkey
- 43: Also at Mersin University, Mersin, Turkey
- 44: Also at Izmir Institute of Technology, Izmir, Turkey
- 45: Also at Ozyegin University, Istanbul, Turkey
- 46: Also at Kafkas University, Kars, Turkey
- 47: Also at Mimar Sinan University, Istanbul, Istanbul, Turkey
- 48: Also at Rutherford Appleton Laboratory, Didcot, United Kingdom
- 49: Also at School of Physics and Astronomy, University of Southampton, Southampton, United Kingdom
- 50: Also at University of Belgrade, Faculty of Physics and Vinca Institute of Nuclear Sciences, Belgrade, Serbia
- 51: Also at Argonne National Laboratory, Argonne, USA
- 52: Also at Erzincan University, Erzincan, Turkey
- 53: Also at Yildiz Technical University, Istanbul, Turkey
- 54: Also at Texas A&M University at Qatar, Doha, Qatar
- 55: Also at Kyungpook National University, Daegu, Korea